

Bayesian Optimization in Language Space: An Eval-Efficient AI Self-Improvement Framework

Enoch Hyunwook Kang*

Foster School of Business, University of Washington

Hema Yoganarasimhan

Foster School of Business, University of Washington

December 5, 2025

Abstract

Large Language Models (LLMs) have recently enabled self-improving AI, i.e., AI that iteratively generates, evaluates, and refines its own outcomes. Recent studies have shown that self-improving AI focusing on prompt optimization (i.e., context engineering) can outperform state-of-the-art reinforcement learning fine-tuned LLMs. Here, their ‘performance’ is typically measured by query efficiency—the number of LLM-generated solution samples required to reach a specified performance threshold. However, in many societal applications, the primary limitation is not *generating* new solutions but *evaluating* them. For instance, evaluating an ad’s effectiveness requires significant human feedback, which is far more costly and time-consuming than generating a candidate ad. To optimize for the evaluation efficiency objective, a natural approach is to extend Bayesian Optimization (BO), a framework proven optimal for evaluation efficiency, to the language domain. However, the difficulty of directly estimating suitable acquisition functions in LLMs’ minds makes this extension challenging. This paper overcomes this challenge by proving that the combination of the simple and widely used BEST-OF-N selection strategy and simple textual gradients (i.e., textual edits from a critic model), statistically emulates the behavior of the gradients on the canonical Upper Confidence Bound (UCB) acquisition function, which induces optimal exploration in terms of evaluation efficiency. Based on this result, we propose TEXTGRAD-BEST-OF-N BAYESIAN OPTIMIZATION (T-BoN BO), a simple and eval-efficient language-space Bayesian optimization framework for AI self-improvement. We also empirically validate T-BoN BO by applying it to automated ad alignment tasks for persona distribution, demonstrating its superior performance compared to popular state-of-the-art baselines. In sum, T-BoN BO is a simple but principled framework for AI self-improving system design that bridges prompt optimization with classical Bayesian optimization.

Keywords: Self-improving AI, Evaluation efficiency, Bayesian optimization, Context Engineering

*Please ask all correspondence to: ehwkang@uw.edu and hemay@uw.edu.

1 Introduction

1.1 Self-improving AI

Data-centric decision making has long relied on a human-driven cycle of historical data analysis, solution proposal, and experimentation. This human-driven iterative approach has supported a wide range of business decisions, ranging from website design [Hauser et al., 2009] to product recommendations [Nandy et al., 2021]. We briefly describe this paradigm using the example of ad-optimization; see the left panel of Figure 1. The process starts with generating a set of ad creatives based on a creative brief. This task is often done by ad agencies or marketers, who rely on their understanding of the product, theories of consumer behavior, market conditions, and feedback from prior ad campaigns. This ad *generation* process typically takes weeks, and serves as the main bottleneck in the iterative ad-optimization process. Once we have a set of candidate ads, the manager moves to *evaluation*, i.e., feeds these ads into advertising platforms or consumer surveys to identify the best performing one, and this step usually takes a few days. Finally, to complete this feedback loop, the manager *analyzes* the performance of the ads from this campaign and uses the insights learned to generate a new slate of candidate ads; and the iterative process continues.

Although effective in many settings, this human-driven workflow suffers from drawbacks. First, the speed with which firms can iterate over this process depends critically on how quickly humans can *generate* new candidate solutions. Historically, generating new candidate solutions (or ads in the case of our example) has been time-consuming, and this step formed a key bottleneck in speeding up the process. Further, there exists no formal framework for how human agents can *analyze* and learn from the performance of prior solutions and leverage them to propose better candidates, and this step is often left to managerial intuition. Indeed, much of the research and managerial focus on data-driven business solutions has largely centered on the *evaluation* step, i.e., given a set of candidate solutions/options, how can we identify the most effective one – and solutions such as A/B tests and Multi-Armed Bandits (MAB) experiments have been proposed and tested [Kohavi et al., 2020, Fiez et al., 2024].

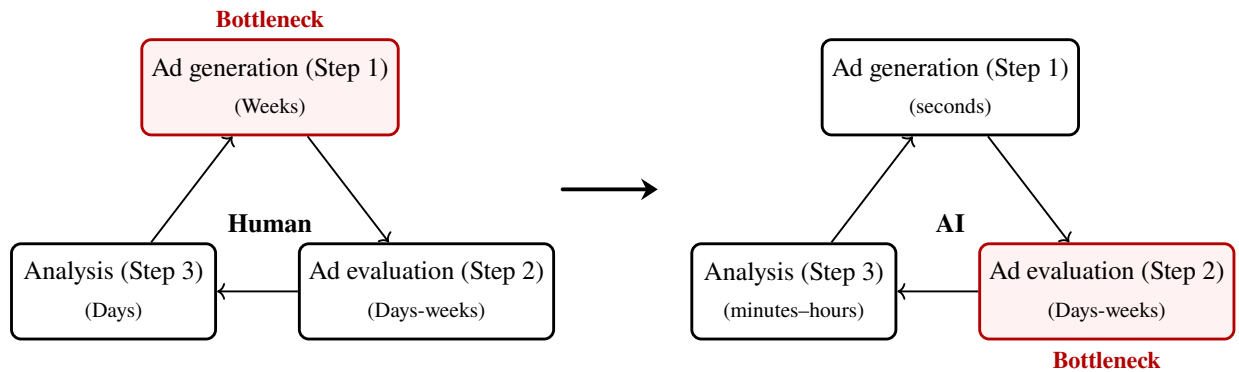


Figure 1: Comparison of human-driven and AI-driven ad self-improvement cycles in digital advertising.

Recent advances in generative AI have begun to transform this human-driven paradigm by providing potential solutions to the issues discussed above. First, candidate generation is fast and scalable with generative

AI models. For example, in the case of digital ads, generative models can produce high-quality creative outputs, including ad copy, images, and complete campaign concepts that adhere to brand guidelines in a matter of minutes [Jansen et al., 2024, Hartmann et al., 2025].¹ Second, Large language Models (LLMs) and related generative systems can now conduct sophisticated data analysis, summarizing performance patterns and identifying potential drivers of success [Ferber et al., 2024, Guo et al., 2024b, Ghosh et al., 2024, Wiedemer et al., 2025], providing a pathway for analyzing historical data and improving candidate solutions. As such, with the new capabilities enabled by AI, the time required for previous data analysis and generation of new candidate solutions are significantly reduced.

Given these developments, there is immense interest in the development and deployment of AI-based automation of the complete generation–evaluation–analysis loop at scale, allowing systems to update themselves continuously in response to emerging data (See right panel of Figure 1). In this loop, generative models produce new solution candidates, data-science agents conduct evaluation of the solution candidates, and multi-modal reasoning LLM-based analytical agents interpret the evaluation results and synthesize insights to guide the next generation step. This type of automated cycle running system is often referred to as the *self-improving AI* or *self-evolving AI* [Mantia et al., 2025, Chen et al., 2025, Silver and Sutton, 2025].

This transformation has an important implication for practice: it dramatically lowers the marginal cost of iteration, making continuous experimentation feasible not only for large firms or organizations with dedicated analytics teams but also for small and medium-sized firms that historically lacked the creative and analytical capacity to run many cycles in parallel. When generation and analysis become cheap and largely automated, even resource-constrained organizations can maintain always-on optimization loops that adapt campaigns to evolving market conditions and consumer responses.

As generation and analysis become increasingly automated and inexpensive in this self-improving loop, the bottleneck in data-centric decision making shifts from proposing and interpreting candidates to *evaluating* them in the real world. Even if analysis can be performed quickly and new candidate solutions can be generated almost instantaneously, each iteration still has to be validated by interacting with the real environment and collecting outcome data. The effective pace of the cycle is therefore governed by evaluation-related constraints such as available traffic, experimentation budgets, and the amount of data required to obtain statistically reliable comparisons among candidates, rather than by generation or analysis speed.

For instance, in digital advertising, even when generating ad creatives via LLM queries is super fast, but evaluating an ad’s effectiveness still requires significant human feedback or large-scale experimentation [Johnson, 2023]. A similar pattern arises in other scientific and engineering domains: protein structures or sequences can be proposed rapidly by models such as AlphaFold [Jumper et al., 2021], but their functional properties must still be confirmed through slow and noisy wet-lab assays; and chip layouts can be generated in silico by systems such as AlphaChip [Goldie et al., 2024], yet rigorous evaluation depends on physical fabrication and benchmarking. As generation and analysis become increasingly automated and inexpensive, the evaluation step thus emerges as the primary bottleneck that limits the overall cadence of self-improvement.

¹Indeed, a substantial share of creatives is now generated by AI, reflecting improvements in both quality and speed [Coffee, 2025, Majic, 2025].

As such, any societal and business AI system we design needs to be *evaluation-efficient*, i.e., reach a high-performing solution using as few costly evaluations as possible, rather than optimizing for a few inexpensive generations.

1.2 Prompt optimization-based self-improving AI

A natural question is, then, how the computer science literature has instantiated self-improving AI in concrete algorithmic frameworks. To date, a central line of success in self-improving AI has arisen in the domain of iterative prompt optimization, where AI agents iteratively refine their own prompts in response to performance feedback. Agrawal et al. [2025] showed that iterative prompt optimization-based self-improving AI can be much more efficient than state-of-the-art model fine-tuning techniques such as GRPO [Liu et al., 2024a]. Specifically, given any limited budget for the number of LLM generation query calls, their proposed iterative prompt optimization method, named GEPA (Genetic-Pareto), outperformed GRPO across their experiments. Those experiments included benchmarks such as complex questions across multiple Wikipedia articles, strict instruction-following under constraints, retrieval-augmented fact verification to support or refute claims, and maintaining answer quality while avoiding privacy leakage.

In all those benchmarks, the primary efficiency metric was *generation efficiency*. i.e., the number of LLM query calls required to generate candidate answers to reach a target performance level. Likewise, prior literature on prompt-based self-improving AI [Agrawal et al., 2025, Zhang et al., 2025, Wang et al., 2025] has focused on measuring efficiency in terms of *generation efficiency*, not evaluation efficiency. Indeed, leading approaches are often specified as procedural heuristic search routines which finds near-optimal solution with small computations, e.g., population-based or random-search-style algorithms that treat prompts as individuals in an evolutionary process or as configurations in a heuristic pipeline. Specifically, they often maintain a pool or batch of prompts, repeatedly generate new variants via LLM-driven mutation, crossover, reflection, or trace-based resampling, score these candidates on held-out data or rollouts, retain the top-performing or Pareto-optimal prompts, and iterate this generate–score–select–mutate loop under a budget of LLM forward passes [Fernando et al., 2024, Guo et al., 2024a, Agrawal et al., 2025, Soylu et al., 2024]. This mirrors the design philosophy of classical evolutionary and heuristic optimization, where the quality of the best solution is assessed as a function of the computation budget rather than the evaluation budget [Nguyen et al., 2016, Ding et al., 2023, Hu et al., 2024, Liu et al., 2024b]. Consequently, evaluation efficiency objective has been largely overlooked in the computer science literature.

However, as we discussed earlier, in self-improving AI for real-world societal and business problems, the primary bottleneck is no longer *generating* new solutions efficiently (generation efficiency) but *evaluating* them efficiently (evaluation efficiency). This shift in the dominant constraint calls for rethinking prompt-optimization-based self-improving AI frameworks so that they explicitly treat evaluation budget as the scarce resource to be allocated and optimized over.

1.3 Research agenda and Challenges

Motivated by the effectiveness of iterative prompt-optimization-based self-improving AI and the overlooked importance of evaluation efficiency in existing frameworks, we now turn to our central question: how can we design a prompt-optimization-based self-improving AI framework that is evaluation-efficient? In addition to evaluation efficiency, we would like the framework to be easy to implement, theoretically grounded, and empirically perform well. However, realizing these desiderata in a unified framework is nontrivial.

The key insight in this paper is that prompt-optimization-based self-improving AI follows a familiar pattern we saw in the optimization framework called *Bayesian Optimization (BO)* [Frazier, 2018, Srinivas et al., 2012, Papenmeier et al., 2025]. This insight is grounded in three observations: First, LLMs learn in-context from previous evaluations [Brown et al., 2020, Coda-Forno et al., 2023, Lu et al., 2024, Cahyawijaya et al., 2024], acting as Bayesian learners [Xie et al., 2021, Wang et al., 2023b, Wakayama and Suzuki, 2025]. Second, we iteratively choose a candidate prompt that generates a candidate solution, observe a noisy performance score associated with this solution, and then decide where to query next. Third, we have to be cognizant of three concerns: (1) we have no closed-form model linking prompts to scores, (2) we need to balance exploration and exploitation when choosing the next candidate solution, and (3) the goal is to optimize for the number of evaluations rather than candidate generation.

BO is a principled framework for tackling such black-box optimization problems with such features. In BO, we build a function called the acquisition function and choose the point with the top of the acquisition function as the next point to evaluate. Among many variants of BO, Upper Confidence Bound (UCB)-BO [Srinivas et al., 2012], a version of BO with UCB acquisition function, is proven to be evaluation-efficient, in the sense that no algorithm can achieve better regret in terms of both simple regret and expected cumulative regret [Whitehouse et al., 2023, Wang et al., 2023a]. Figure 2 illustrates the procedure of UCB-BO.

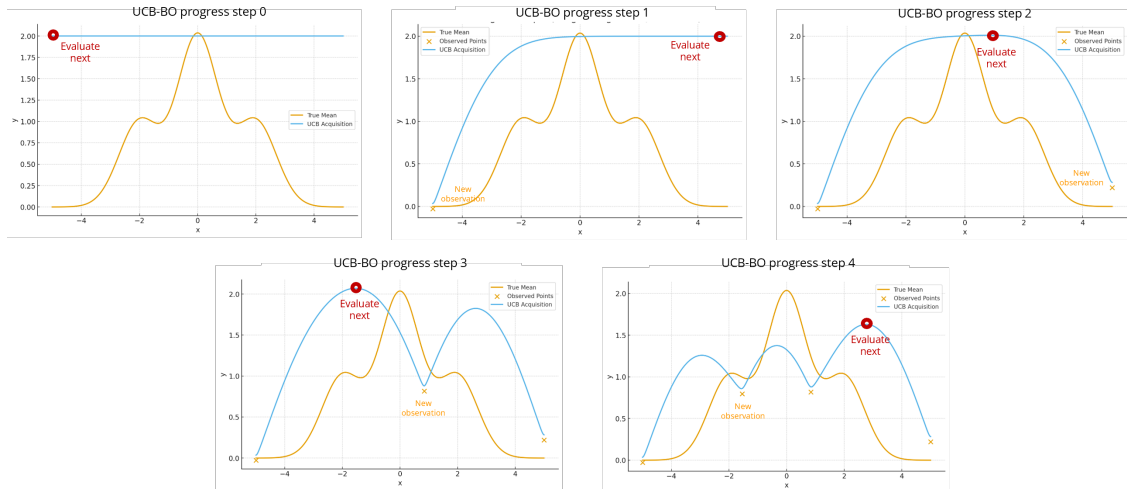


Figure 2: An example of a non-parallel UCB-BO procedure for four optimization steps. At each step, we choose the maximum (or multiple local maxima in the parallel UCB-BO) of the blue UCB function as the next point to evaluate.

As you can see from Figure 2, the UCB acquisition function is often non-concave. To resolve this issue, in practice, we often use parallel gradient-based UCB-BO [Wilson et al., 2018], where we 1) start from multiple initial points and take gradients to find a set of local optima, and 2) choose those local optima as the points to evaluate next. Parallel gradient-based BO has shown surprising empirical effectiveness for high-dimensional problems [Papenmeier et al., 2025].

Building on the key insight, we propose to achieve evaluation efficiency by casting iterative prompt optimization-based self-improving AI as parallel gradient-based UCB Bayesian optimization in language space. At each iteration, we treat the prompts from the previous round as initialization points and take gradient steps to ascend the UCB acquisition function toward its local optima. We then select which prompts to evaluate from among these local optima. After each evaluation round, the LLM and its associated critic models implicitly update a surrogate belief over prompt quality via in-context learning and corresponding UCB, analogous to the posterior update in classical Bayesian optimization.

However, there are two challenges we need to overcome.

- **Challenge 1– Lack of gradient functions**

In prompt spaces, the notion of a gradient is ill-defined because they lack the inner-product structure of a Hilbert space required to measure the directions and magnitudes of change [Young, 1988]. Thus, we first need to define a meaningful notion of a “gradient” in the domain of text. Although one might consider going around this challenge by embedding the prompt first, taking the gradient there, and reverting the prompt, this strategy runs into the well-known soft-to-discrete projection problem, where such reverted prompts break any clean correspondence between infinitesimal moves in embedding space and interpretable edits of the underlying natural-language prompt [Cui et al., 2025].

- **Challenge 2 – Taking gradients for UCB**

Second, even if we can define meaningful gradients in prompt space, we do not have direct access to the underlying UCB acquisition function whose gradient we would like to follow. The surrogate posterior over prompt quality that induces UCB lives implicitly in the LLM, rather than as an explicit Gaussian-process-style model that exposes closed-form posterior means, variances, and their derivatives. Consequently, standard gradient-based BO techniques that differentiate the UCB constructed from a known surrogate cannot be applied naively: we must design a mechanism that elicits UCB-like, optimism-in-the-face-of-uncertainty behavior using only black-box text interactions and critic feedback, without ever computing the UCB function or its gradient in closed form.

In this paper, our goal is to address the above challenges and build an evaluation-efficient self-improving AI that optimally balances exploration and exploitation in the language space.

1.4 Proposed Method

We propose a simple, evaluation-efficient iterative prompt-optimization framework, called **TEXTGRAD-BEST-OF-N BAYESIAN OPTIMIZATION (T-BoN BO)**, that adapts parallel gradient-based UCB-BO for prompt optimization based self-improving AI (Figure 3), addressing both of the challenges discussed earlier.

To solve the first challenge, T-BoN BO builds on the recently proposed **TEXTGRAD** [Yuksekgonul et al.,

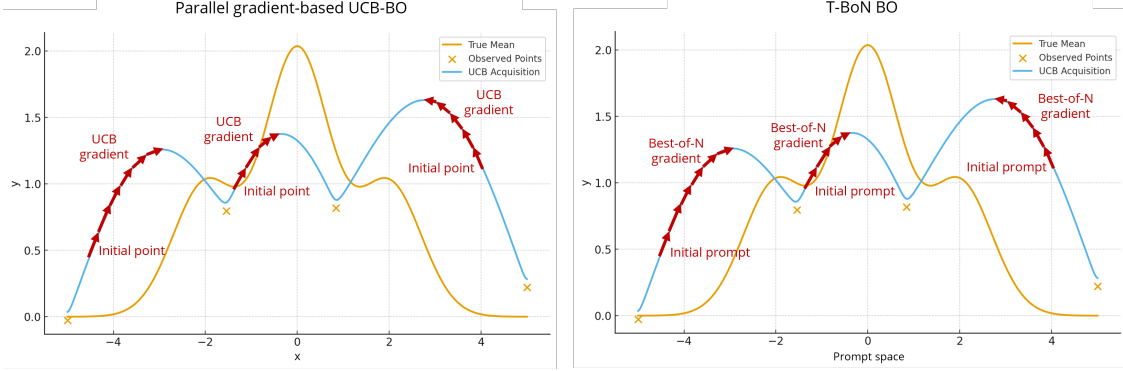


Figure 3: Gradient steps of parallel gradient-based BO (Left image) and those of T-BoN BO (Right image). T-BoN BO extends parallel gradient-based BO to the language space.

2025] framework that adapts gradient descent to discrete text by asking an external auxiliary LLM *critic* to propose targeted edits that improve a candidate; applying these edits induces a local, directional update, i.e., a “textual gradient”, in language space. This makes gradient-style search feasible without continuous relaxations or mapping the LLM prompts to the embedding space. For instance, consider an ad creative generation prompt for an image model: “A simple photo of a plant-based burger on a white plate.” A critic LLM might suggest: “Make the burger appear delicious, and show it being enjoyed at a barbecue.” Incorporating this edit yields: “A photorealistic image of a juicy plant-based burger with grill marks, served at a vibrant summer barbecue with friends.” This change is analogous to following a gradient direction—small, constructive, and aligned with improving performance according to the evaluation signal. Yuksekogonul et al. [2025] show that textual gradients based on their approach enable consistent improvements across diverse scientific domains such as code-completion benchmarks, improving accuracy on graduate-level QA datasets, optimizing drug-like molecules, and refining radiotherapy planning for clinical objectives. These results establish textual gradients as an effective surrogate for numerical gradients when optimizing systems that operate in language space.

To address the second challenge, T-BoN BO chooses the prompt to evaluate next via a series of textual gradients which are selected under the Best-of-N principle [Snell et al., 2024], resulting in the gradient direction we call *Best-of-N gradient*. Moving in the textual gradient direction suggested by the critic exploits the expected improvement implied by past results but ignores uncertainty in those expectations. Therefore, it does not climb the UCB acquisition function. Best-of-N gradient bakes in *exploration* into the choice of gradient direction by adopting an optimism-based rule in the spirit of UCB’s optimism-in-the-face-of-uncertainty principle: it samples multiple local textual edits and moves along the direction the LLM judges most promising, i.e., the Best-of-N candidate. That is, the Best-of-N gradient is designed to simulate the implicit UCB acquisition gradient in language space.

We now briefly describe our T-BoN BO algorithm. At each optimization iteration, in Step 1 (meta-reflection phase), we use the critic model to analyze the history of previously evaluated solutions and their scores, and update a meta-reflection that summarizes what has tended to work well or poorly. In Step 2

(Best-of- N textual-gradient phase), we perform a sequence of Best-of- N gradient updates from the current prompt. That is, for each gradient step, (i) we propose N textual-gradient edits that transform the current prompt into N candidate prompts, (ii) each candidate prompt is passed to a solution-generation model to produce a corresponding candidate solution, (iii) conditioned on the meta-reflections, the critic model predicts which candidate solution is most likely to perform best, and (iv) we set the prompt associated with this predicted-best solution as the new current prompt. After iterating Step 2, we obtain a refined prompt and its associated solution to evaluate. In Step 3 (evaluation phase), we evaluate this solution to get a scalar score, which T-BoN BO then uses to update its history and meta-reflection for subsequent optimization steps.

1.5 Theoretical Guarantees and Empirical Evaluation

We provide theoretical guarantees on the performance of our approach. We formally show that, under mild regularity conditions, the Best-of- N gradient over locally sampled textual edits induces, in probability, ascent directions of the UCB acquisition function with an exploration parameter $\beta_N = \Theta(\sqrt{\ln N})$ (Theorem 2). In other words, T-BoN BO emulates parallel gradient-based UCB Bayesian Optimization in the implicit embedding space induced by the LLM, even though it operates purely in language space and does not construct an explicit surrogate or uncertainty model. Since UCB-BO is known to achieve sublinear regret and optimal evaluation-efficiency guarantees, T-BoN BO inherits these theoretical properties up to constant factors and approximation error stemming from textual gradients. In sum, we formally establish that T-BoN BO is theoretically equivalent to the parallel gradient-based implementation of Bayesian Optimization with the Upper Confidence Bound (UCB) acquisition function [Srinivas et al., 2012, Wilson et al., 2018], which is proven to be evaluation-efficient [Whitehouse et al., 2023, Wang et al., 2023a]. This equivalence establishes T-BoN BO as a valid, eval-efficient, parallel gradient-based Bayesian optimization procedure in the language space.

In addition to its theoretical efficiency, T-BoN BO is simple and easy to implement since it does not require any explicit uncertainty modeling, embeddings, or Gaussian process surrogates. We now demonstrate the empirical performance of our approach using a series of numerical experiments. Concretely, we instantiate T-BoN BO in a digital advertising setting, where the goal is to iteratively refine image-generation prompts for ad creatives so as to maximize ad responsiveness for a population of customers. We test and measure how well and how fast a method optimizes for (i.e., aligns with) the preference distribution induced by LLM-based simulation of personas in the Digital Twins persona dataset called Twin-2k-500 [Toubia et al., 2025].² We demonstrate that T-BoN BO significantly outperforms strong state-of-the-art baselines such as BEST-OF- N [Snell et al., 2024] and GEPA [Agrawal et al., 2025] in terms of evaluation efficiency, i.e., reaching fixed performance with a smaller number of steps. Specifically, we show that:

- T-BoN BO, the proposed evaluation efficient framework, achieves nearly twice more improvements from BEST-OF- N baselines compared to GEPA [Agrawal et al., 2025], the state-of-the-art prompt optimization-

²While LLM-based persona simulation can be biased and may not reflect real-world human behavior [Li et al., 2025a, Peng et al., 2025], it still induces a valid preference distribution. As such, it can serve as a valid benchmark on which we can compare the performance of different AI-based optimization methods.

based self-improving AI algorithm, which outperforms GRPO [Liu et al., 2024a], the state-of-the-art reinforcement learning fine-tuning algorithm.

- T-BoN BO outperforms the state-of-the-art baseline even when we simulate preferences without any persona information, i.e., when the evaluator is a single LLM judge with no auxiliary context.

Together, these results show that T-BoN BO can reach good performance both in settings where there is significant heterogeneity in the preferences of the target population as well as in settings with homogeneous preferences.

In sum, our paper makes four main contributions to the literature on AI, optimization, and data-driven decision making. First, from a conceptual perspective, we identify evaluation efficiency as the key objective to optimize in self-improving AI design in societal and business systems. Second, we propose T-BoN BO, a purely text-based self-improving AI framework that combines textual-gradient search with Best-of- N selection to automate and optimize business and marketing decisions (e.g., ad creatives, product descriptions). Third, we provide theory showing that Best-of- N over locally sampled textual edits selects, in probability, ascent directions of the UCB acquisition with exploration weight $\beta = \Theta(\sqrt{\ln N})$; thus, we prove that T-BoN BO emulates gradient-based UCB and inherits evaluation-efficiency guarantees. Finally, we demonstrate empirical gains on automated ad-alignment across eight scenarios: T-BoN BO improves faster and attains higher final scores compared to strong baselines, including BEST-OF-64 and GEPA, and remains effective both in settings with and without contextual information.

The rest of the paper is organized as follows. Section 2 discusses the related literature. Section 3 formalizes the AI system and its objective, along with self-improving algorithms. Section 4 describes the concept of *Best-of- N gradient* and proves that it theoretically emulates the gradient of the UCB acquisition function. Section 5 introduces the main self-improving AI algorithm proposed in this paper, T-BoN BO. Sections 6 and 7 empirically demonstrate T-BoN BO’s effectiveness on ad-alignment tasks versus strong baselines. Finally, Section 8 concludes with a discussion of implications and limitations.

2 Related Literature

Our paper relates and contributes to multiple streams of literature, including the literature on AI and LLMs in computer science, the operations literature on optimization, and the marketing literature on ad optimization. We now discuss each one below.

The literature on self-improving AI has often been motivated by an observation: the progress in AI based only on human data is hitting limits, so AI must create and learn from its own data. In other words, powerful AI “should have their own stream of experience that progresses, like humans, over a long time-scale” [Silver and Sutton, 2025]. That is, we need to design the self-improving AI that iteratively 1) generate data of outcomes, evaluate outcomes with grounded signals, and 2) self-tune the three knobs –*models*, *tools*, and *prompts*– in the system to achieve long-term objectives under real-world feedback [Wang et al., 2025]. Here, tuning models is about altering language models’ input-output correspondences [Huang et al., 2023, Lee et al., 2023, Acikgoz et al., 2025]; tuning tools is about specifying the tools the AI has access to, including memory tools [Hou et al., 2025, Ouyang et al., 2025, Qiu et al., 2025]; tuning prompts is about engineering prompts in

the model’s context window, including system messages, task instructions, constraints, schemas, and few-shot exemplars [Zhou et al., 2022, Khattab et al., 2023, Yang et al., 2024, Yuksekgonul et al., 2025, Agrawal et al., 2025, Zhang et al., 2025, Wang et al., 2025]. In this paper, we focus on studying self-improving systems based on tuning prompts.

Our paper also relates to the literature on relating LLMs to Bayesian Optimization (BO). A series of papers focuses on applying LLM to enhance BO for numerical optimization problems. Liu et al. [2024c] and Cissé et al. [2025] focus on leveraging LLMs’ contextual understanding and few-shot learning capabilities to improve BO’s efficiency, enabling better warm-starting and surrogate modeling; Aglietti et al. [2025] uses an LLM to discover new acquisition functions for Bayesian optimization. The LLM writes candidate acquisition function formulas as code, which are evaluated on various optimization problems. Conversely, Singh et al. [2025] applies BO to enhance LLM’s internal behavior to boost the model’s zero-shot and few-shot performance. In contrast to these papers, our paper focuses on considering the prompt optimization problem that arises in formulating LLM-based self-improving AI system design as a Bayesian Optimization problem. In line with this focus, Schneider et al. [2025] and Kong et al. [2025] formulate prompt optimization among the fixed set of candidate prompts as Bayesian optimization. While Schneider et al. [2025] utilizes ideas from adversarial bandits, Kong et al. [2025] feeds each prompt text into an embedding model, and the GP surrogate operates on those fixed embedding features to guide selection. In contrast to these approaches, our work focuses on self-improving AI that actively generate new candidate prompts as the process proceeds, rather than pre-specifying a fixed set of candidate prompts.

In terms of method evaluation benchmarks, our paper relates to the methodological literature on ad optimization in digital marketing. A series of papers focused on the efficient execution of ad evaluation, i.e., iteratively improving ad choice efficiently given a fixed set of candidate ads. Schwartz et al. [2017] adopts Thompson Sampling with a hierarchical general linear model for a real display advertising campaign for a financial-services firm, which purchased display advertising across 59 websites. Geng et al. [2020] partitions JD.com’s platform users into disjoint sub-populations and applies a contextual Thompson sampling algorithm to maximize the expected advertiser payoff. Aramayo et al. [2023] developed a contextual Thompson sampling algorithm to dynamically determine the list of house ads to display on the homepage of an electronic retailer to maximize the accumulated click-through rate of the ads. Ba et al. [2022] used parametric Thompson Sampling, where a parametric structure links features (media, audience attributes) to conversion likelihood to optimally allocate ad-media and target-audience combinations in high-dimensional settings with low success rates. The main difference between bandit-based papers and ours is the existence of a pre-defined set of candidate arms. Self-improving AI focuses on creating new solutions by analyzing previous results. On the other hand, bandit methods aim to balance exploration of a predefined set of candidate ads optimally. More broadly, there is also a difference in problem scope. Self-improving AI iterates among three steps: generation, evaluation, and analysis. In contrast, bandit methods focus on efficiently executing the evaluation step. Indeed, an AI self-improvement framework’s evaluation step may employ a bandit method to improve efficiency further.

3 Setup and Background

3.1 The optimization objective.

Consider a system designer’s decision-making problem, where she chooses a prompt Π for the LLM-based AI system Φ .³ We call $\Phi(\Pi)$ the ‘system outcome’ of Φ corresponding to a prompt Π . In a digital marketing setting, Φ is an image generation AI, and $\Phi(\Pi)$ is the ad generated by the prompt Π . As a system, $\Phi(\Pi)$ has inputs and corresponding outputs. Specifically, $\Phi(\Pi)$ maps the input space \mathcal{X} to a distribution over an output space \mathcal{Y} . For each $x \in \mathcal{X}$, we denote by $y(\Phi(\Pi), x)$ the random \mathcal{Y} -valued vector output of the system at input x . In a digital marketing setting, input $x \in \mathcal{X}$ is a platform user, and a realization of $y(\Phi(\Pi), x)$ represents that user’s reaction (e.g., clicks, conversions, spend) to the ad $\Phi(\Pi)$.

The distribution of inputs over \mathcal{X} may depend on the prompts set Π . For example, in a digital marketing setting, a recommender system on the ad platform determines which users are shown the ad $\Phi(\Pi)$. To capture such dependences, we denote the input distribution over \mathcal{X} by $\mathcal{D}_{\mathcal{X}}(\Pi)$.

To evaluate the output, we use a scoring rule: a function $r : \mathcal{Y} \rightarrow [0, 1]$ that assigns a scalar effectiveness score to each $y \in \mathcal{Y}$. In the digital marketing example, r is a marketer-defined function that maps observed user responses (clicks, conversions, spend) to a normalized scalar effectiveness score.

Our optimization objective is to discover the prompt Π^* that maximizes the objective function

$$J(\Pi) := \mathbb{E}[r(y(\Phi(\Pi), x))]. \quad (1)$$

Note that J cannot be optimized by directly computing gradients, because the input distribution $\mathcal{D}_{\mathcal{X}}(\Pi)$ can shift with Π ; even when $J(\Pi)$ is differentiable with respect to Π and y ’s randomness is not dependent on Π , we have:

$$\nabla_{\Pi} J(\Pi) = \underbrace{\mathbb{E}[\nabla_{\Pi} r(y(\Phi(\Pi), x))]}_{\text{model term}} + \underbrace{\mathbb{E}[r(y(\Phi(\Pi), x)) \nabla_{\Pi} \log d_{\Pi}(x)]}_{\text{distribution term}}, \quad (2)$$

where d_{Π} is the density of $\mathcal{D}_{\mathcal{X}}(\Pi)$. Since d_{Π} and $\nabla_{\Pi} \log d_{\Pi}(x)$ are unobservable, we cannot compute gradients from observed rewards. This motivates the use of an external LLM that can analyze prior data and propose directions for improvement without explicitly computing gradients, leading to self-improving AI algorithms we describe below that iteratively optimize for J .

3.2 Self-improving AI algorithm

Given a scoring rule r , a *self-improving AI algorithm* \mathcal{A} optimizes $J(\Pi) := \mathbb{E}[r(y(\Phi(\Pi), x))]$ through iteratively analyzing the previous history, proposing a new prompt, and observing its noisy score. Formally, starting from the initial prompt Π_0 , a self-improving AI algorithm proceeds in discrete optimization iterations, indexed by $t = 1, 2, \dots$; at the beginning of iteration t , the algorithm has access to the history of past prompts

³LLM-based AI systems can also be modified by tuning the LLM’s internal parameters using LLM fine-tuning methods such as GRPO [Liu et al., 2024a]. In this paper, we focus on prompt optimization, which fixes those internal parameters throughout.

and their observed scores, then selects a new prompt Π_t , deploys the corresponding system outcome $\Phi(\Pi_t)$, and receives a score feedback on its performance. We define the score s_t of prompts Π_t as the empirical average reward at t , i.e.,

$$s_t := \frac{1}{L} \sum_{l=1}^L r\left(y\left(\Phi(\Pi_t), x_t^{(l)}\right)\right), \quad x_t^{(l)} \sim \mathcal{D}_{\mathcal{X}}(\Pi_t), \quad (3)$$

where L denotes the number of input samples $x_t^{(l)}$ we evaluate for each t . Note that we compare the performance of algorithms in terms of the progress of s_t across iterations t .

Definition 1 (Self-improving AI algorithm). *Fix a system Φ and a scoring rule r . For each iteration $t \geq 1$, let the history of past evaluations be*

$$H_{t-1} := \{(\Pi_\tau, c_\tau, s_\tau)\}_{\tau=0}^{t-1} \quad (4)$$

where s_τ is the empirically evaluated score of Π_τ , defined as

$$s_t = \frac{1}{L} \sum_{l=1}^L r(y(\Phi(\Pi_t), x_t^{(l)})), \quad x_t^{(l)} \sim \mathcal{D}_{\mathcal{X}}(\Pi_t). \quad (5)$$

Then, a self-improving AI algorithm is defined as function \mathcal{A} that, at each iteration t , maps the history H_{t-1} to a new prompt Π_t , i.e.,

$$\Pi_t = \mathcal{A}_t(H_{t-1})$$

The goal of \mathcal{A} is to choose the sequence $(\Pi_t)_{t \geq 0}$ so as to optimize the objective $J(\Pi)$, equivalently to drive the sequence of empirical scores $(s_t)_{t \geq 1}$ upward over iterations in expectation.

Operationally, given access to the history H_{t-1} , a self-improving AI algorithm \mathcal{A} goes through following three steps each iteration t :

1. *Analysis*: The critic LLM analyzes the previous history H_{t-1} .
2. *Generation*: The critic LLM proposes the next prompts Π_t based on the analysis.
3. *Evaluation*: The system outcome $\Phi(\Pi_t)$ is deployed, and its performance is measured, yielding a score s_t .

The new observation is added to the history: $H_t = H_{t-1} \cup \{(\Pi_t, c_t, s_t)\}$.

3.3 Bayesian Optimization (BO)

As discussed in Section 1, we would like to formulate self-improving AI as parallel gradient-based UCB-BO. At its core, BO maximizes an unknown and expensive-to-evaluate objective function under a limited evaluation budget. Formally, consider a black-box function $f : \mathcal{Z} \rightarrow \mathbb{R}$, where in our setting f corresponds to the system-level objective $J(\Pi)$ over prompts. BO maintains a *surrogate model*, typically a Gaussian Process (GP) or another probabilistic regressor defined on \mathcal{Z} , that summarizes current beliefs about f . For any candidate $z \in \mathcal{Z}$, the surrogate yields a posterior mean $\mu(z)$ and an associated uncertainty measure $\sigma(z)$.

In BO, the following evaluation point is selected by choosing the point that maximizes an *acquisition function* $A(z)$ constructed from $\mu(z)$ and $\sigma(z)$, rather than by directly maximizing $\mu(z)$. Acquisition functions encode an explicit trade-off between *exploitation* (preferring points with high predicted value) and *exploration* (preferring points with high uncertainty). A widely used choice is the Upper Confidence Bound (UCB) acquisition function

$$A_\beta(z) = \mu(z) + \beta \sigma(z), \quad (6)$$

where the exploration parameter $\beta > 0$ controls the strength of the exploration term [Srinivas et al., 2012]. Intuitively, UCB acquisition function gives a positive bonus to unexplored areas in addition to the posterior mean. This allows us to follow the “optimism in the face of uncertainty” principle, which is known to trade off exploration and exploitation effectively. Indeed, UCB-BO is an optimal algorithm for achieving evaluation efficiency, in the sense that no algorithm can achieve better regret guarantees [Wang et al., 2023a, Whitehouse et al., 2023] (See Web Appendix E for a detailed theoretical discussion of BO.)

In practice, since the maxima of the UCB acquisition function are often not available in a closed form, we typically use parallel gradient-based BO with the UCB acquisition function [Wilson et al., 2018]. In parallel gradient-based BO, we start from multiple initial points and take gradients from them to climb up the UCB acquisition function to find its local maxima. We then choose the points to evaluate among the local maxima (Figure 3).

In our setting, we do not construct an explicit $\mu(\cdot)$ and $\sigma(\cdot)$ (and their corresponding surrogate model and acquisition function) for the prompt space; instead, we interpret $\mu(\cdot)$ and $\sigma(\cdot)$ as implicit beliefs within the LLM and design our method to emulate parallel gradient-based UCB in this implicit space. Textual gradient [Yuksekgonul et al., 2025] is designed to elicit gradients for $\mu(\cdot)$ in the prompt space without explicitly modeling those beliefs within the LLM. However, what we want is not gradients for $\mu(\cdot)$; we want gradients for $A_\beta(z)$, the UCB acquisition function.

4 Best-of-N gradient and Theory

As discussed in Section 1, a core challenge in casting self-improving AI as parallel, gradient-based UCB Bayesian optimization in the space of prompts is the absence of an explicit acquisition function (e.g., UCB) and its gradient. As we discussed earlier, textual gradients [Yuksekgonul et al., 2025] can guide the prompt toward the highest expected improvement based on immediate feedback, as a textual gradient elicits the gradient of the posterior mean $\nabla \mu(x)$. However, following the posterior mean’s gradient rather than UCB’s is a purely exploitative strategy that often leads to suboptimal local maxima.

In this section, we propose that a gradient direction we call *Best-of-N gradient*, which generates N stochastic textual gradients and selecting the most promising candidate via a Best-of- N mechanism, can elicit the gradient of the UCB acquisition function within LLM’s mind without explicitly constructing the LLM’s implicit posterior mean and the associated uncertainty.

To operationalize the Best-of-N gradient, we should first formalize the requisite capabilities of the external

Large Language Model, which we designate as the *Critic LLM*.

4.1 Critic LLM.

Let Π denote a prompt and $c = \Phi(\Pi)$ denote the corresponding system outcome. We define the history of optimization up to iteration t as $H_t = \{(\Pi_\tau, c_\tau, s_\tau)\}_{\tau \leq t}$. Then we define the Critic LLM, M_{critic} , as an LLM that can conduct the operations of the following four distinct operators:

1. *Pairwise Judge Operator*: A function that compares two outcome c_1 and c_2 , given a reflection R and predicts which outcome will yield a higher true score:

$$\text{PAIRWISEJUDGE}(c_1, c_2; R, M_{\text{critic}}) \in \{c_1, c_2\} \quad (7)$$

2. *Reflection Operator*: A function that compresses the entire history into a natural-language summary of rules or guidelines:

$$R_t = \text{METAREFLECT}(H_t; M_{\text{critic}}) \quad (8)$$

3. *Textual Gradient Operator*: A stochastic function that generates a textual gradient δ (e.g., “Make the lighting warmer”) intended to improve the prompt:

$$\delta \sim \nabla_{\text{text}}(\Pi; R) \quad (9)$$

4. *Rewrite Operator*: A deterministic function that maps a prompt Π and an edit δ to a new prompt Π' :

$$\Pi' = \text{Apply}(\Pi, \delta; M_{\text{critic}}) \quad (10)$$

In the digital-marketing example, these correspond to an LLM’s ability to (1) compare two ad creatives and predict which will perform better [Calderon et al., 2025], (2) examine past performance data and derive guidelines for effective ads in context [Jiang et al., 2024, Ferber et al., 2024], (3) propose prompt improvements based on those guidelines [Yuksekgonul et al., 2025, Li et al., 2025b], and (4) apply prompt improvements to get the new prompt.

4.2 Best-of- N gradient

The notion of a Best-of- N gradient builds on the widely used Best-of- N strategy for test-time alignment, where an LLM trades additional inference-time (test-time) compute for higher-quality outputs by sampling multiple candidate generations and then selecting the one that appears most aligned with a downstream objective [Snell et al., 2024, Beirami et al., 2024]. In the standard Best-of- N strategy for prompting, an LLM generates N candidate prompts, a generation model produces N candidate outcomes, and a reward model selects the highest-scoring one. While effective for choosing a single output, our goal is to improve the

prompt itself to ensure sustained performance improvement. To achieve this, we introduce the concept of the *Best-of-N Gradient*. Instead of sampling N candidate prompts directly, we sample N distinct *textual gradients* (directions of improvement). By applying these N textual edits to the current prompt and selecting the LLM-as-a-judge-predicted most promising candidate solution (Best-of-N), we aim to identify the textual gradient direction for the implicit acquisition function. The procedure operates as follows:

- 1) *Textual gradient generation*: Using M_{critic} , query the textual-gradient operator N independent times to obtain a set of small edits:

$$\delta^{(i)} \sim \nabla_{\text{text}}(\Pi; R, M_{\text{critic}}), \quad i = 1, \dots, N. \quad (11)$$

- 2) *Candidate prompt generation*: Apply each edit to the current prompt to generate N candidate prompts:

$$\Pi^{(i)} = \text{Apply}(\Pi, \delta^{(i)}; M_{\text{critic}}), \quad i = 1, \dots, N. \quad (12)$$

- 3) *Candidate system outcome generation*: Generate the corresponding system outcomes for each candidate prompt:

$$c^{(i)} = \Phi(\Pi^{(i)}), \quad i = 1, \dots, N. \quad (13)$$

- 4) *Best-of-N selection*: Select the best candidate by iteratively applying PAIRWISEJUDGE operation using M_{critic} as LLM-as-a-judge. We define this selection as BEST-OF-N operation, which induces the index i^* as the best one among N :

$$i^* = \text{BEST-OF-N}(\{(\Pi^{(i)}, c^{(i)})\}_{i=1}^N; R, M_{\text{critic}}). \quad (14)$$

The resulting prompt $\Pi^{(i^*)}$ represents the update step taken by the Best-of-N Gradient.

For the Best-of-N selection, we employ the pairwise tournament [Liu et al., 2025]. First, the N candidates are permuted to produce randomly chosen tournament matches. Each match compares two outcomes by querying M_{critic} for a head-to-head judgment (For the prompt, please refer to Figure 11 in Appendix A). illustrates the prompt example for ad generation tasks. To mitigate noise, the comparison is repeated K times (typically an even number to evenly swap orders to remove positional bias [Shi et al., 2024], and ties are broken by random. Winners advance round by round until only the final winner remains. Given the final winner’s index i^* , we define $(\Pi_{t,g}^j, c_{t,g}^j) := (\Pi_{t,g}^{j,(i^*)}, c_{t,g}^{j,(i^*)})$ and carry it forward for the next gradient step $g + 1$.

4.3 Theory: Best-of-N gradient’s Asymptotic Equivalence to UCB gradient

In this section, we prove that the Best-of- N over textual gradients selects, in probability, the ascent direction of the UCB acquisition with exploration weight β scaling as $\Theta(\sqrt{\ln N})$ (Theorem 2). What allows us to do

rigorous theoretical analysis is that LLM prompt embeddings are invertible and bi-Lipschitz: LLM’s prompt embeddings are known to be injective, and therefore invertible [Nikolaou et al., 2025]; LLM embeddings are Lipschitz [Tang et al., 2025], implying they are bi-Lipschitz. Hence, small textual edits can be represented as small changes in the embedding space and vice versa. This enables us to map changes in prompts to changes in embeddings in Euclidean space, and later bring the theoretical guarantees back in the prompt space.

Intuitive explanation.

Denote x to be an embedding of a prompt. Pick a small radius $\varepsilon > 0$ around x and sample N nearby edits $x_i = x + \varepsilon u_i$ with u_i on the unit sphere. Score each point

$$Y_i = \mu(x_i) + \xi_i \sigma(x_i), \quad \xi_i \text{ i.i.d. sub-Gaussian and independent of } \{u_i\}. \quad (15)$$

Let $M_N = \max_i \xi_i$ and $q_N = F^{-1}(1 - 1/N)$. Since $M_N \simeq q_N$ and $q_N = \Theta(\sqrt{\ln N})$, Best-of- N acts like picking the sampled x_i with the largest

$$\mu(x_i) + q_N \sigma(x_i). \quad (16)$$

On the small sphere around x the function $A_\beta(x') = \mu(x') + \beta \sigma(x')$ has a single best direction. Call it v_β . Draw a narrow cone around v_β . Then, with a large enough N , at least one u_i lands in that cone with high probability. The winner comes from that cone. Set $\beta = q_N$. Then Best-of- N behaves like UCB with weight β : it picks the sampled point most similar to the A_β best direction.

Rigorous derivation.

Let \mathcal{M} be the set of syntactically valid prompts. Suppose that there exists a text embedding $E : \mathcal{M} \rightarrow \mathbb{R}^d$, where $x := E(\Pi) \in \mathbb{R}^d$ is the embedding of a prompt $\Pi \in \mathcal{M}$. We first state the assumptions motivated by how language model embeddings behave in practice, and then state the main theorem, Theorem 2.

At each gradient step of T-BoN BO, we sample edits that correspond to $u_1, \dots, u_N \stackrel{\text{i.i.d.}}{\sim} \rho$ on the embedding space $\subset \mathbb{R}^d$, where ρ is assumed to have a density bounded below by a positive constant with respect to surface measure. Assumption 1 implies that small textual edits induce near-linear moves in \mathbb{R}^d , consistent with the recent findings that prompt embeddings preserve phrase similarity under small changes [Reimers and Gurevych, 2019, He et al., 2025, Tang et al., 2025, Nikolaou et al., 2025].

Assumption 1 (Embedding map and edit realization). *For the current prompt Π with $x = E(\Pi)$, constants $C < \infty$ and $\varepsilon_0 > 0$ such that for every unit vector $u \in \mathbb{R}^d$ and every $\varepsilon \in (0, \varepsilon_0]$ the edit operator Apply realizes a first-order move:*

$$E(\text{Apply}(\Pi, \varepsilon u)) = x + \varepsilon u + r(\varepsilon, u), \quad \sup_{\|u\|=1} \|r(\varepsilon, u)\| \leq C \varepsilon^2. \quad (17)$$

Next, the assumption 2 is a standard regularity/technical condition: let’s call a function $f : \mathbb{R}^d \rightarrow \mathbb{R}$ is $C^{1,1}$ if it is continuously differentiable and its gradient is Lipschitz: $\exists L < \infty$ such that $\|\nabla f(y) - \nabla f(z)\| \leq$

$L\|y - z\|$ for all y, z .

Assumption 2 (μ, σ are of $C^{1,1}$). *Let $\mu(x)$ and $\sigma(x)$ denote the mean and standard deviation of the evaluation variable Y at embedding x . We assume μ, σ are $C^{1,1}$ locally. We use $g = \nabla\mu(x)$ and $h = \nabla\sigma(x)$.*

Assumption 3 specifies a heteroscedastic sub-Gaussian model for candidate scores (with i.i.d. mean-zero, unit-variance, unbounded-support noise independent of the sampled directions) and an ideal Best-of- N choice oracle.

Assumption 3 (Noise model and choice oracle). *Let $\{\xi_i\}_{i=1}^N$ be i.i.d. mean-zero, unit-variance, Gaussian random variables with unbounded support, independent of $\{u_i\}$. For candidates $x_i := x + \varepsilon u_i$ we observe*

$$Y_i = \mu(x_i) + \sigma(x_i) \xi_i, \quad (18)$$

and the Best-of- N oracle returns $i^ \in \arg \max_{i \in [N]} Y_i$.*

Assumption 4 (Small-step regime and limit order). *We take limits with $N \rightarrow \infty$ first, then $\varepsilon \downarrow 0$.*

Lemma 1 (Gaussian maxima and spacing [Vershynin, 2018]). *Let ξ_1, \dots, ξ_N be i.i.d. mean-zero, unit-variance Gaussian, $M_N = \max_{i \leq N} \xi_i$, S_N the second largest, and $q_N := F^{-1}(1 - 1/N)$ the $(1 - 1/N)$ -quantile of ξ_1 . Then $q_N = \Theta(\sqrt{\ln N})$, $M_N - q_N \rightarrow 0$ in probability, and $M_N - S_N = O_p(1/q_N)$.*

Theorem 2 (Best-of- N asymptotically induces a UCB gradient direction). *Under Assumptions 1-4, define $\beta_N := q_N$ from Lemma 1. Let $i^* \in \arg \max_i Y_i$ and set $\hat{u}_N := u_{i^*}$. Define the step*

$$\Delta x^{(N)} := \mathbb{E}(\text{Apply}(\Pi, \varepsilon \hat{u}_N)) - x = \varepsilon \hat{u}_N + r(\varepsilon, \hat{u}_N). \quad (19)$$

Then, with the limit order $N \rightarrow \infty$ first and $\varepsilon \downarrow 0$ second,

$$\frac{\Delta x^{(N)}}{\|\Delta x^{(N)}\|} = \hat{u}_N \xrightarrow{p} \frac{\nabla A_{\beta_N}(x)}{\|\nabla A_{\beta_N}(x)\|} = \frac{g + \beta_N h}{\|g + \beta_N h\|}. \quad (20)$$

Moreover,

$$A_{\beta_N}(x + \Delta x^{(N)}) \geq A_{\beta_N}(x) + \varepsilon \|\nabla A_{\beta_N}(x)\| - o_p(\varepsilon). \quad (21)$$

5 TextGrad-Best-of-N Bayesian Optimization (T-BoN BO)

We now describe the self-improving AI framework proposed in this paper: TEXTGRAD-BEST-OF-N BAYESIAN OPTIMIZATION (T-BoN BO). As discussed in Section 1, T-BoN BO is designed to implement parallel gradient-based UCB-BO in the discrete space of natural language (Figure 3). Specifically, T-BoN BO implements the parallel gradient-based UCB-BO that reuses the final gradient point as the initialization for the next iteration. Therefore, each initial point gives rise to a *trajectory*: a sequence of candidate points obtained by repeatedly taking gradient-ascent steps and evaluations starting from that initialization.

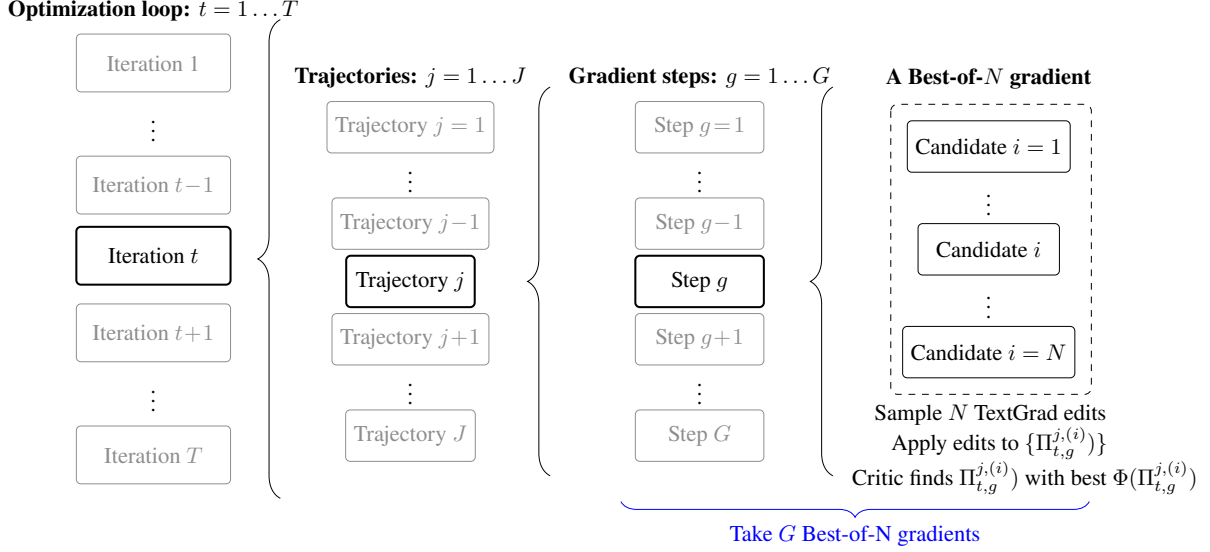


Figure 4: Visual summary of T-BoN BO (Algorithm 1) with T iterations, J trajectories, and G Best-of- N gradients per each iteration and trajectory.

Algorithm. Throughout T number of optimization iterations, T-BoN BO runs J trajectories in parallel, starting from a set of initial prompts, denoted $\{\Pi_0^j\}_{j=1}^J$. At each iteration and a trajectory, we fix the hyperparameters: the number of candidates per gradient step (N) and the number of gradient steps per iteration (G).

At iteration $t = 0$, it starts from evaluating $\{\Pi_0^j\}_{j=1}^J$, i.e., the initial systems $\{c_0^j = \Phi(\Pi_0^j)\}_{j=1}^J$, on $\{\mathcal{D}_{\mathcal{X}}(\Pi_0^j)\}_{j=1}^J$ to obtain initial scores $\{s_0^j\}_{j=1}^J$. The history is then initialized as $H_0 = \bigcup_{j=1}^J \{(\Pi_0^j, c_0^j, s_0^j)\}$. The shared reflection is initialized as $R_0 = \emptyset$.

At each iteration t , for each trajectory $j \in \{1, \dots, J\}$, we set $\Pi_{t,0}^j$ as Π_{t-1}^j and proceed as follows:

1. **Best-of- N gradients.** (Detailed in Section 4.2) For each trajectory j , repeat steps 1) – 4) for $g = 1, \dots, G$:

- 1) Textual gradient generation: From the current prompt $\Pi_{t,g-1}^j$, query the textual-gradient generation operator $\nabla_{\text{text}}(\Pi_{t,g-1}^j; R_{t-1}, M_{\text{critic}})$ independently N times to obtain textual gradients $\{\delta_{t,g}^{j,(i)}\}_{i=1}^N$.
- 2) Candidate prompt generation: Apply each textual gradient $\delta_{t,g}^{j,(i)}$ to $\Pi_{t,g-1}^j$ for all i to get $\{\Pi_{t,g}^{j,(i)}\}_{i=1}^N$.
- 3) Candidate system outcome generation: Produce the system outcomes $\{c_{t,g}^{j,(i)} := \Phi(\Pi_{t,g}^{j,(i)})\}_{i=1}^N$.
- 4) Best-of- N selection: Find the best of $\{(\Pi_{t,g}^{j,(i)}, c_{t,g}^{j,(i)})\}_{i=1}^N$ using the critic and the shared reflection R_{t-1} , and set the winner as $(\Pi_{t,g}^j, c_{t,g}^j)$.

2. **Evaluation.** For each trajectory j ,

- 1) Set $c_t^j = c_{t,G}^j$ and $\Pi_t^j = \Pi_{t,G}^j$.

2) Evaluate c_t^j to get the score $s_t^j = \text{Eval}(c_t^j, \mathcal{D}_{\mathcal{X}}(\Pi_t^j))$, where

$$\text{Eval}(c_t^j, \mathcal{D}_{\mathcal{X}}(\Pi_t^j)) := \frac{1}{L} \sum_{l=1}^L r(y(c_t^j, x_t^{j,(l)})), \quad x_t^{j,(l)} \sim \mathcal{D}_{\mathcal{X}}(\Pi_t^j), \quad (22)$$

3) Given $\{(\Pi_t^j, c_t^j, s_t^j)\}_{j=1}^J$, append it to the shared history H_{t-1} to form H_t .

4) If $s_t^j > s_{t-1}^j$, keep (Π_t^j, c_t^j) . Otherwise, revert trajectory j to the previous state: $(\Pi_t^j, c_t^j) = (\Pi_{t-1}^j, c_{t-1}^j)$ and set $s_t^j = s_{t-1}^j$.

For 4), we follow Yuksekogonul et al. [2025] and adopt a simple acceptance rule that controls progress: if $s_t \geq s_{t-1}$, the new candidate is adopted; otherwise, the system rolls back to the previous iteration’s outcome, i.e., $(\Pi_{t-1}, c_{t-1}, s_{t-1})$. After evaluation of all trajectories, $\{(\Pi_t^j, c_t^j, s_t^j)\}_{j=1}^J$ are appended to the history H_{t-1} to form H_t .

3. Shared Meta-reflection.

At the end of each iteration t , we update the global reflection

$$R_t \leftarrow \text{METAREFLECT}(H_t; M_{\text{critic}})$$

using the aggregated history from all trajectories for use at iteration $t+1$. Here, $\text{METAREFLECT}(H_t; M_{\text{critic}})$ compresses the full history H_t of prompts, generated system outcomes, and evaluation results into a natural language reflection R_t . R_t consists of a small set of actionable rules. In the ad generation example, those rules may take the form “emphasize social context,” “avoid cluttered backgrounds,” or “prefer warm lighting.” This reflection serves as a global memory; in subsequent iterations, the critic LLM takes this reflection as a part of its context when generating textual gradients. (For the prompt used for meta-reflection, see Figure 12 in Appendix A).

There are many ways to construct a reflection from past results. In our experiments, following Li et al. [2025b], we instruct the critic model M_{critic} to compare the five lowest- and five highest-performing outcomes from previous iterations (or, when fewer than ten are available, all outcomes)⁴, identify recurring visual and textual patterns, and distill them into a concise set of actionable rules.

After T optimization steps, the sequence of best-performing outcomes $\{c_t^{j^*}\}_{t=1}^T$, where $j_t^* := \text{argmax}_j s_t^j$, is reported as the algorithm’s result.

Note that T-BoN BO takes $N \times G$ generation of prompt/outcome candidates before each evaluation. This careful selection of a prompt/outcome candidate to evaluate is the key to evaluation efficiency in T-BoN BO: it deliberately trades inexpensive generation compute for fewer evaluations.

Algorithm 1: T-BoN BO

Input: System Φ ; $\{\Pi_0^j\}_{j=1}^J$; critic M_{critic} ; candidates per step N ; gradient steps G ; iterations T ; J trajectories

Output: Optimized triples $\{(\Pi_T^j, c_T^j, s_T^j)\}_{j=1}^J$

```

1 for  $j = 1$  to  $J$  do
2    $c_0^j \leftarrow \Phi(\Pi_0^j)$ ;
3    $s_0^j \leftarrow \text{Eval}(c_0^j, \mathcal{D}_{\mathcal{X}}(\Pi_0))$ ;
4    $H_0 \leftarrow \{(\Pi_0^j, c_0^j, s_0^j)\}$ ,  $R \leftarrow \emptyset$ ;
5 end
6 for  $t = 1$  to  $T$  do
7   for  $j = 1$  to  $J$  do
8      $\Pi_{t,0}^j \leftarrow \Pi_{t-1}^j$ ;
9     for  $g = 1$  to  $G$  do
10      for  $i = 1$  to  $N$  do
11         $\delta_{t,g}^{j,(i)} \leftarrow \nabla_{\text{text}}(\Pi_{t,g-1}^j; R, M_{\text{critic}})$ ;
12         $\Pi_{t,g}^{j,(i)} \leftarrow \text{Apply}(\Pi_{t,g-1}^j, \delta_{t,g}^{j,(i)})$ ;
13         $c_{t,g}^{j,(i)} \leftarrow \Phi(\Pi_{t,g}^{j,(i)})$ ;
14      end
15       $(\Pi_{t,g}^j, c_{t,g}^j) \leftarrow \text{BEST-OF-N}(\{(\Pi_{t,g}^{j,(i)}, c_{t,g}^{j,(i)})\}, R_{t-1}, M_{\text{critic}})$ ;
16    end
17     $c_t^j \leftarrow c_{t,G}^j$ ,  $\Pi_t^j \leftarrow \Pi_{t,G}^j$ ;
18     $s_t^j \leftarrow \text{Eval}(c_t^j, \mathcal{D}_{\mathcal{X}}(\Pi_t))$ ;
19     $H_t \leftarrow H_{t-1} \cup \{(\Pi_t^j, c_t^j, s_t^j)\}$ ;
20    if  $s_t^j < s_{t-1}^j$  then
21       $\Pi_t^j \leftarrow \Pi_{t-1}^j$ ,  $c_t^j \leftarrow c_{t-1}^j$ ,  $s_t^j \leftarrow s_{t-1}^j$ ;
22    end
23  end
24   $R_t \leftarrow \text{METAReflect}(H_t)$ ;
25 end
26 return  $\{c_t^{j*}\}_{t=1}^T$ , where  $j_t^* := \text{argmax}_j s_t^j$ 

```

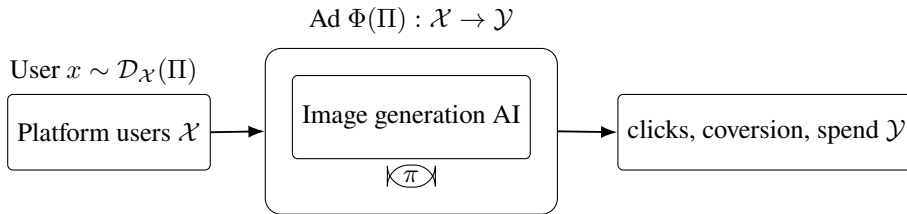


Figure 5: An ad generation AI system Φ and prompt $\Pi = \langle \pi \rangle$.

6 Case Study: Ad Optimization in Digital Marketing

In this section, we present a case study on how ad platforms can use T-BoN BO for ad optimization and automate the ad generation, analysis, and evaluation cycle. Given an a priori fine-tuned image generation AI

⁴Limiting the number of outcomes in the critic model’s context window helps mitigate context rotting [Hong et al., 2025].

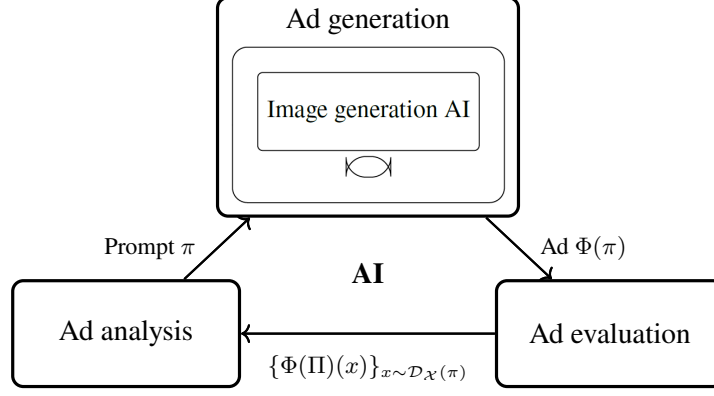


Figure 6: A self-improving AI implemented on the ad generation AI system in Figure 5.

model that is aligned with its client’s brand, the objective is to efficiently refine the prompts for ad generation to better align with the users’ preference distribution.

6.1 Problem definition

Formally, define the brand fine-tuned ad-generation AI system as Φ , whose behavior is controlled by a prompt Π (Figure 5). For a given prompt Π , we write $\Phi(\Pi)$ for the corresponding ad creative shown on the ad platform. As a system, $\Phi(\Pi)$ maps the input space \mathcal{X} (potential ad viewers on the platform) to a distribution over the output space \mathcal{Y} (observable ad responses). For each $x \in \mathcal{X}$, we denote by $y(\Phi(\Pi), x)$ the random \mathcal{Y} -valued output of the system at input x . In a digital marketing setting, x is a platform user, and a realization of $y(\Phi(\Pi), x)$ represents that user’s reaction (e.g., clicks, conversions, spend) to the ad $\Phi(\Pi)$. When a user $x \in \mathcal{X}$ is shown the ad creative $\Phi(\Pi)$, we observe an outcome $y \in \mathcal{Y}$, which is a realization of $y(\Phi(\Pi), x)$.

As discussed earlier, the distribution of exposed users depends on the ad $\Phi(\Pi)$ and therefore on the prompt Π . We denote by $\mathcal{D}_{\mathcal{X}}(\Pi)$ the unknown distribution of users x who are shown the ad generated from Π when the ad $\Phi(\Pi)$ is run on the platform.

To evaluate system performance, a marketer pre-defines a scoring rule $r : \mathcal{Y} \rightarrow [0, 1]$ that maps observed user responses (clicks, conversions, spend) to a normalized effectiveness score. The ad optimization objective of the agency for a given client and campaign can then be written as

$$J(\Pi) := \mathbb{E}[r(y(\Phi(\Pi), x))], \quad (23)$$

where the expectation is taken over $x \sim \mathcal{D}_{\mathcal{X}}(\Pi)$ and any additional randomness in $y(\Phi(\Pi), x)$.

The self-improving ad system built by the agency can therefore be viewed as an iterative algorithm that searches over prompts π in order to maximize $J(\pi)$ while minimizing the number of costly ad evaluations on the platform (Figure 6). At iteration t , a candidate prompt π_t is selected, the corresponding ad creative $\Phi(\pi_t)$ is generated, and the campaign is (conceptually) exposed to a batch of users $\{x_t^{(l)}\}_{l=1}^L \sim \mathcal{D}_{\mathcal{X}}(\pi_t)$. The

empirical evaluation

$$s_t := \frac{1}{L} \sum_{l=1}^L r(y(\Phi(\pi_t), x_t^{(l)})) \quad (24)$$

serves as a noisy estimate of $J(\pi_t)$ and is fed back into the optimization algorithm (T-BoN BO) to update the history H_t and the meta-reflection R_t .

6.2 Application of T-BoN BO

We now describe how the general T-BoN BO framework in Section 5 is instantiated for ad agency’s ad optimization problem. Specifically, we focus on the parallel version of T-BoN BO (Algorithm 1), where J optimization trajectories start from different initial prompts and run simultaneously.

Initialization. The decision-maker/platform starts from initial prompts $\{\pi_0^j\}_{j=1}^J$, i.e., prompts already in use or high-quality baselines provided by humans. (e.g., “A simple, photorealistic image of a plant-based burger patty.”⁵) For each initial prompt π_0^j , the system generates an ad $\Phi(\pi_0^j)$ and obtains an initial score s_0^j by deploying the ad and observing outcomes. These tuples $\{(\pi_0^j, \Phi(\pi_0^j), s_0^j)\}_{j=1}^J$ form the initial history H_0 for the parallel T-BoN BO procedure.

Best-of- N textual-gradient steps. Within each optimization iteration t , T-BoN BO refines each trajectory’s prompt π_{t-1}^j through G Best-of- N textual-gradient steps (Figure 4). For a given trajectory j and inner step g , the critic model M_{critic} (a large language model such as Gemini 2.5 Flash) receives as context: (i) the current prompt $\pi_{t,g-1}^j$, (ii) the current meta-reflection R_{t-1} , and (iii) a short description of the brand and campaign scenario. Conditioned on this context, it proposes N small natural-language edits

$$\delta_{t,g}^{j,(1)}, \dots, \delta_{t,g}^{j,(N)} \sim \nabla_{\text{text}}(\pi_{t,g-1}^j; R_{t-1}, M_{\text{critic}}), \quad (25)$$

which form the textual gradients. Each edit is then applied to the current prompt to obtain N candidate prompts

$$\pi_{t,g}^{j,(i)} \leftarrow \text{Apply}(\pi_{t,g-1}^j, \delta_{t,g}^{j,(i)}; M_{\text{critic}}), \quad i = 1, \dots, N. \quad (26)$$

These textual gradients correspond to small, directed moves in language space that, according to the critic’s judgment, are likely to increase ad effectiveness. For example, conditioned on the reflection R_{t-1} (e.g., “social occasions and visible grill marks tend to perform better than plain pack shots”), the critic M_{critic} may propose the following textual-gradient candidates:

1. *Emphasize social context and enjoyment:* “Show the burger being enjoyed at an outdoor barbecue with friends, not alone on a plate.”

⁵Note that in the experiments in Section 7, we use WORST5-OF-N prompts as initial starting points, which are higher-quality, much more detailed initial prompts; See Appendix A.

2. *Highlight sensory appeal and indulgence*: “Make the patty look extra juicy with clear grill marks, a toasted bun, and melty toppings.”
3. *Make sustainability salient but secondary*: “Subtly include eco-friendly cues (like a small ‘plant-based’ tag or greenery in the background) without overpowering the food.”

Each of these textual gradients $\delta^{(i)}$ is then applied to the original prompt to produce candidate prompts. For example, applying the first gradient yields the prompt:

“A photorealistic image of a juicy plant-based burger with grill marks, served at a vibrant summer barbecue with friends, everyone smiling and reaching for food.”

Applying the second gradient yields the prompt:

“A close-up, photorealistic shot of a plant-based burger with deep grill marks, a toasted brioche bun, melty vegan cheese, fresh toppings, and steam rising to suggest warmth and juiciness.”

To select the next prompt that will go forward to the next gradient step among N candidate prompts $\{\pi_{t,g}^{j,(i)}\}_{i=1}^N$, T-BoN BO applies the Best-of- N choice rule over the N corresponding candidate ads $\{c_{t,g}^{j,(i)}\}_{i=1}^N$. Following Liu et al. [2025], we implement Best-of- N via a pairwise tournament: in each match, the critic model M_{critic} compares two creatives side by side and predicts which will perform better, given the campaign goals and the current meta-reflection R_{t-1} (see Figure 11 in Appendix A). After multiple randomized pairwise comparisons, the winner $c_{t,g}^j$ and its corresponding prompt $\pi_{t,g}^j$ are carried forward to the next gradient step. Repeating this expansion-and-selection process for $g = 1, \dots, G$ yields the refined prompt π_t^j and ad $\Phi(\pi_t^j)$ for trajectory j at iteration t .

Evaluation as the costly step. Once all G gradient steps are completed, T-BoN BO performs a single expensive evaluation for each trajectory by deploying the ad $\Phi(\pi_t^j)$ and computing the score s_t^j . In the real ad-agency use case, this evaluation step would correspond to running the creative in an A/B test, multi-armed bandit experiment, or survey-based study, and mapping the resulting performance metrics to a scalar score via the scoring rule r . The new triple $(\pi_t^j, \Phi(\pi_t^j), s_t^j)$ is appended to the history H_t , and a simple acceptance rule is applied: if s_t^j fails to improve upon s_{t-1}^j , the trajectory rolls back to $(\pi_{t-1}^j, \Phi(\pi_{t-1}^j), s_{t-1}^j)$.

Meta-reflection shared across trajectories. After all J trajectories have been evaluated at iteration t , the algorithm updates the global meta-reflection $R_t = \text{METAREFLECT}(H_t)$, as in Section 5. Concretely, M_{critic} is prompted to review a subset of the best- and worst-performing ads and prompts in H_t and to summarize the key patterns and rules that distinguish successful creatives from unsuccessful ones (see Figure 12 in Appendix A). For example, the reflection may emphasize that scenes with social eating and visible grill marks perform better than isolated product shots, or that emphasizing “satisfying” and “juicy” yields higher effectiveness scores. This reflection is then injected into the context of subsequent textual-gradient generation and Best-of- N comparisons, allowing all trajectories to share accumulated knowledge even though they explore different regions of the prompt space.

Reported outcome. After T iterations, the system returns the sequence of best-performing ads $\{c_t^{j^*}\}_{t=1}^T$, where $j_t^* = \arg \max_j s_t^j$ is the trajectory that achieves the highest score at iteration t .

7 Experiments

We validate the empirical effectiveness of the proposed T-BoN BO framework for a real-world digital marketing problem described in 6. Specifically, we examine if and how much T-BoN BO improves outcomes under a fixed evaluation budget compared to state-of-the-art baselines.

7.1 Evaluation Module using Persona data and LLM-based Simulation

To evaluate how well an ad performs on the target population and improve prompts, we need a target population and a way to measure the preferences of that population for a given ad. There are many ways to do this, such as field experiments, consumer surveys, or simulated responses from a pre-defined target population. In our experiments, we use LLM-generated preferences over the Twin-2k-500 persona distribution provided by Toubia et al. [2025]. An important advantage of using this persona distribution is that it allows us to test the performance of different algorithms fast without the need for large-scale field experiments or expensive surveys.⁶

This dataset includes the data of 2,058 U.S. adults answering 500 survey questions spanning demographics, personality, cognitive ability, economic preferences, classic heuristics-and-biases tasks, and a pricing study. These survey questions of each persona are passed to a multi-modal LLM (Gemini 2.5 Flash) as context so that the LLM can simulate the ad effectiveness for the persona.⁷ We divided the Twin-2k-500 personas into 80% (1647 personas) for the training set and 20% (411 personas) for the test set. Every time we evaluate an ad during the algorithm (i.e., training stage), we randomly sample 200 personas from the training set and simulate the ad’s effectiveness for them. Every time we want to test an ad, such as a final ad output from the algorithm, we simulate its effectiveness for all the test set personas.

7.2 Experiment Setup

We consider eight synthetic ad campaign scenarios that cover a diverse range of products across distinct categories, defined by the creative brief that outlines the strategic and creative direction for each scenario. (For the creative brief for each scenario, see Appendix B.)

- Scenario 1: “GreenBite,” a new plant-based burger patty.
- Scenario 2: “AuraSonics X1,” high-end, noise-canceling wireless earbuds.
- Scenario 3: “Odyssey E-SUV,” a new all-electric family SUV.
- Scenario 4: “Oasis Eco-Lodge,” a secluded, luxury resort with beautiful natural surroundings.
- Scenario 5: “Momentum,” a mobile-first banking app for freelancers and the gig economy.

⁶Note that naive field deployment cannot be used to test the relative performance of algorithms since an algorithm’s measured advantage would be a mix of its own effect and distributional effects induced by the ad platform’s ad targeting systems.

⁷While LLM-based persona simulation is often biased and does not reflect real-world human behavior [Li et al., 2025a, Peng et al., 2025], it still induces a valid preference distribution for which, as a benchmark, we would like to see how well a method can optimize.

- Scenario 6: “MindGarden,” a subscription-based meditation and mindfulness app.
- Scenario 7: “Aeterno,” a classic, automatic Swiss-made wristwatch with a heritage design.
- Scenario 8: “SyncFlow,” a project management and collaboration software platform for remote teams.

For each scenario, from its creative brief, we generated 64 high-quality initial prompts that were used as input to the state-of-the-art image generation AI model named Imagen 4 ⁸ to generate the initial 64 high-quality ads. (For prompts, see Figure 13 and 14 in Appendix A.) To maintain a rigorous baseline, we made the 64 initial prompts detailed enough to yield strong ads. This ensures that the algorithm’s subsequent improvements are not explained as trivial quality gains from having initial under-specified prompts. That is, the measured improvements are attributed to the algorithm’s ability to align ads with the underlying persona distribution better.

When simulating an ad’s effectiveness for a persona, we ask the LLM (with the prompt in Figure 7) what the ad’s “effectiveness”⁹ for the persona will be, with the score of [1, 2, 3, 4, 5]. Here, the score of one is the least effective, and the score of five is the most effective. As the LLM’s internal assignment of probability for the scores is available as ‘logprobs’¹⁰, we use them to calculate the mean score, and consider it as the evaluation score of the ad for the persona (which is a fraction number like 3.41), instead of considering the actual response score from the LLM (which is an integer number among 1-5). We then take the average of the evaluation scores for the personas to get the final evaluation score of the ad.

Among the initial ads, we identified the best initial ad, which we call **BEST-OF-64**, and the worst five initial ads, which we call **WORST5-OF-64**, by running a best-arm identification bandit algorithm [Russo, 2016] by alternating the best-arm identification objective and worst 5-arm identification objective for evaluations of 5,000 sequential random samples from the training persona set.

7.3 Baselines

As baselines, we consider the performance of two popular state-of-the-art algorithms. One is the **BEST-OF-64** [Snell et al., 2024] baseline, which is one of the most popular and well-performing test-time alignment methods that has been reported to outperform reinforcement learning fine-tuning methods under large enough N [Gao et al., 2023, Mudgal et al., 2023, Eisenstein et al., 2023, Beirami et al., 2024]. Specifically, the test persona set-based evaluation result for the Best-of-64 ad (identified above in Section 7.2 using training persona set) was used as the **BEST-OF-64** baseline. We also evaluated the ads in **Worst5-of-64** in the same way and took the mean of their scores to obtain the **WORST5-OF-64** baseline.

Another baseline is GEPA (Genetic-Pareto) [Agrawal et al., 2025]. As discussed earlier, this reflective and evolutionary prompt evolution algorithm has recently demonstrated superior performance compared

⁸See Vertex AI’s description (<https://console.cloud.google.com/vertex-ai/publishers/google/model-garden/imagen-4.0-generate-preview-06-06>) for details.

⁹The vagueness of the term “effectiveness” constitutes an evaluation distribution induced by LLM-persona based on what LLM ‘thinks’ about the term, which we target to align the algorithms with. That is, as long as we consistently query the same LLM to predict “effectiveness” using the same prompt, such vagueness is justified.

¹⁰See Vertex AI’s logprobs description (<https://cloud.google.com/vertex-ai/generative-ai/docs/model-reference/inference#logprobs>) for details.

Persona prompt for simulating ad effectiveness.

```
PERSONA DATA: {  
Which part of the United States do you currently live in? [Answer]  
What is the highest level of schooling or degree that you have completed? [Answer]  
... (Many other survey questions and answers) ...  
Suppose you were given 5 and had to offer to another (anonymous) person a way to split the money... [Answer]  
... (Many other survey questions and answers) ...  
}  
  
AD IMAGE: [image]  
  
TASK: Return only one item from ["1","2","3","4","5"] for ad effectiveness.  
Effective Score Scale Definition:  
1: Extremely Unlikely. The persona would actively ignore or be annoyed by this ad.  
2: Unlikely. The persona would likely scroll past without a second thought.  
3: Mediocre. It is hard to decide whether the persona would click or don't click.  
4: Likely. The persona is intrigued and has a good chance of clicking to learn more.  
5: Extremely Likely. The persona is the ideal target; a click is almost certain.  
No explanation. Just the score.
```

Figure 7: Persona simulation prompt for the digital marketing problem.

to GRPO [Liu et al., 2024a], a state-of-the-art reinforcement fine-tuning technique. GEPA keeps a set of candidate prompts, and samples a prompt to mutate based on its evaluation result for a problem (in our case, a persona) set they call the Pareto set. A Pareto set stores ‘important’ problems. Since we randomly sample personas from the training persona set, we cannot store specific personas and retrieve them later. Therefore, we instead use the version of GEPA that 1) randomly samples a persona and 2) mutates all candidate prompts equally and throws away the old prompts to avoid unbounded growth of the candidate set.

For the experiment, we run five-trajectory ($J = 5$) parallel T-BoN BO and GEPA starting from Worst5-of-64, i.e., the worst five initial prompts we identified in Section 7.2. This starting point allows us to attribute observed gains to the algorithms rather than to favorable starting prompts. We test if T-BoN BO outperforms the BEST-OF-N baseline and GEPA baseline throughout the optimization process. For both T-BoN BO and GEPA, we ran 10 optimization steps, evaluating 200 randomly sampled personas per step (2,000 total persona evaluations). We used a multi-modal LLM (Gemini-2.5-Flash) to serve as the critic model for both T-BoN BO and GEPA.

7.4 Results and Analysis

Trend analysis

Figure 8 plots how much T-BoN BO, GEPA, and BEST-OF-N improved their performance from the initial WORST5-OF-N score across eight scenarios. (For the detailed data used to generate this plot, refer to Table 2 and 3 in Appendix C.) At each step (the x -axis), the performance score (the y -axis) is the average of eight scenarios’ mean evaluation score for the testing persona set. For example, the step-2 score is the average of the eight step-2 mean evaluation scores. As the figure illustrates, both T-BoN BO and GEPA improve consistently across steps, with T-BoN BO demonstrating faster early gains and achieving a significantly better final performance than GEPA. Notably, by the third step on average, which is equivalent to 600 persona

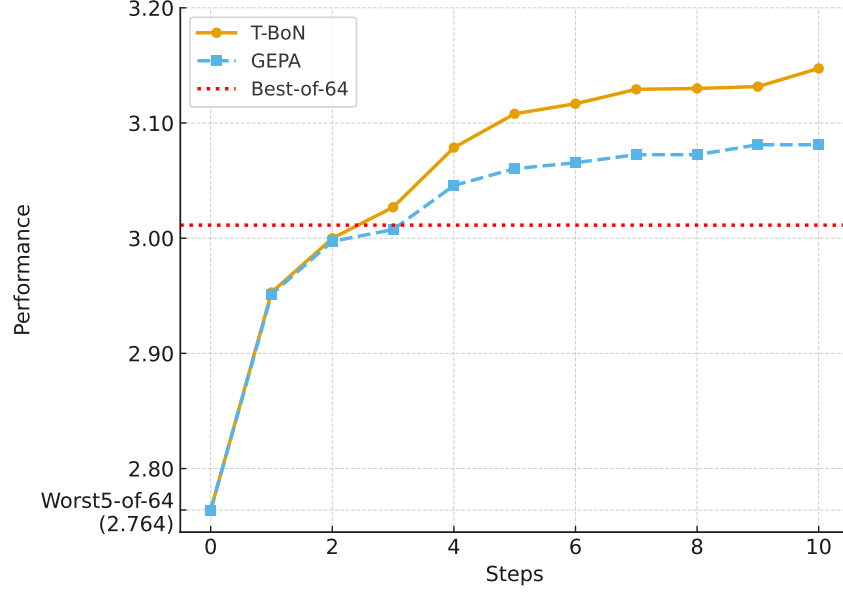


Figure 8: Progress comparison of T-BoN BO and GEPA with BEST-OF-64 baseline. T-BoN BO implements parallel T-BoN BO with $J = 5$. The performance score (the y -axis) is the average of eight scenarios' mean evaluation score for the testing persona set. Since it is the mean of means, we don't plot the standard errors.

evaluations, T-BoN BO and GEPA both outperform the BEST-OF-64 baseline.

Statistical analysis

<i>Model</i>			
$\text{score} = \alpha + \beta_1 \mathbf{1}\{t = 10\} + \beta_2 \mathbf{1}\{\text{TBoN}\} \mathbf{1}\{t = 10\} + \text{persona FE} + \text{scenario FE} + \varepsilon$			
<i>Effect</i>	Estimate	Std. err	T-stat
β_1 : GEPA gain ($t = 10$) from WORST5-OF-64	0.3168***	0.0325	9.752
β_2 : T-BoN BO gain - GEPA gain ($t = 10$) from WORST5-OF-64	0.0743***	0.0248	2.991
$\beta_1 + \beta_2$: T-BoN BO gain ($t = 10$) from WORST5-OF-64	0.3911***	0.0355	11.011
<i>Summary statistics</i>			
Observations		13,152	
Personas		411	
Scenarios		8	

Notes: Two-way cluster-robust standard errors. * $p < 0.10$, ** $p < 0.05$, *** $p < 0.01$.

Table 1: Two-way fixed effect (TWFE) analysis result with persona and scenario fixed effects with two-way clustered SEs [Cameron et al., 2011]. Standard error of $\beta_1 + \beta_2$ was computed using Delta method.

In addition to the aggregate trend analysis provided in Figure 8, we now provide statistical evidence that T-BoN BO indeed outperforms the GEPA. For this, we conducted a Two-way Fixed Effect (TWFE) analysis using T-BoN BO and GEPA's final ($t = 10$) scores to compare the effectiveness of each method rigorously.

Specifically, we consider the following TWFE model:

$$\text{score} = \alpha + \beta_1 \mathbf{1}\{t = 10\} + \beta_2 \mathbf{1}\{\text{TBoN}\} \mathbf{1}\{t = 10\} + \text{persona FE} + \text{scenario FE} + \varepsilon. \quad (27)$$

where $\mathbf{1}\{t = 10\}$ is the indicator variable of whether it is $t = 0$ (GEPA and T-BoN BO’s initial starting point, i.e., WORST5-OF-64 score) or $t = 10$ (GEPA and T-BoN BO’s final score), β_1 is the GEPA’s gain from WORST5-OF-64 after $t = 10$, β_2 is the T-BoN BO’s advantage over GEPA after $t = 10$, and $\beta_1 + \beta_2$ is the T-BoN BO’s gain from WORST5-OF-64 after $t = 10$. The unobserved residual ε is assumed to follow the normal distribution. To remove potential correlation among unobserved residuals within the same persona or scenario, we conducted a cluster-robust Two-way Fixed Effect (TWFE) analysis with two-way clustering [Cameron et al., 2011, Cameron and Miller, 2015]. The result of TWFE analysis is shown in Table 1. As we can see, both of T-BoN BO’s gain and GEPA’s gain from the starting point (WORST5-OF-64) after $T = 10$ are statistically significant. In addition, we conclude that T-BoN BO has a significant 23.5% more gain in score compared to GEPA’s gain.

Qualitative analysis

The significant gains of GEPA and T-BoN BO can be interpreted as demonstrating their ability to align with the persona distribution. However, such significance can also be easily gained by starting from a poor starting point, i.e., a poor WORST5-OF-N prompt and corresponding ad image. One way to check whether this happens is to compare the quality of the prompts; we provide them in Appendix A to demonstrate that this is not the case. Another qualitative approach is to compare the generated ad images and verify whether the differences among ads are in quality or in the message and representation. Figure 9 compares the ad images of the baseline methods. As we can see, there is no clear visual quality difference among those ad images; the differences are mainly in the ad’s message and how it is represented. This supports the claim that T-BoN BO and GEPA improvements from WORST5-OF-N demonstrated in Figure 8 are attributed to alignment, not trivial quality gains from correcting poor or under-specified prompts.

7.5 Ablation study

The main experiment in Section 7.1-7.4 evaluates the candidate ad at each iteration as the mean of scores across 411 personas (20% of the persona data in Twin-2k-500 [Toubia et al., 2025]) that were injected into the LLM’s context. Each persona consists of a large amount of information, with 500 survey questions accounting for around 50,000 tokens. Would T-BoN BO still outperform strong state-of-the-art baselines when the LLM receives less persona context information?

To test this, we ran a no-persona ablation experiment in which the evaluator is a single LLM (Gemini 2.5 Flash) with no auxiliary persona context. Concretely, at each iteration, we present only the ad image candidate to LLM judge (Gemini 2.5 Flash) together with the same 1–5 effectiveness rubric, set temperature to 0, and compute the same scalar score as the log-probability-weighted expectation over $\{1, \dots, 5\}$ as before.¹¹ This

¹¹With temperature = 0, the judge’s output is deterministic for a fixed image and rubric; the logprob vector is still available, so the expected score is stable across repeated calls.








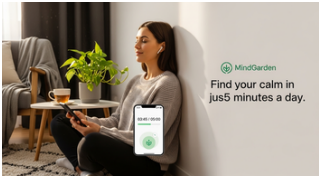




	GreenBite (Plant-based patty)	MindGarden (Meditation app)	AuraSonics X1 (Noise-canceling earbuds)
WORST5-OF-64 (starting point)			
	Score: 2.672	Score: 2.670	Score: 2.765
BEST-OF-64			
	Score: 2.898	Score: 2.930	Score: 2.934
GEPA (after T=10)			
	Score: 3.046	Score: 3.068	Score: 3.028
T-BoN BO (after T=10)			
	Score: 3.168	Score: 3.132	Score: 3.104

Figure 9: T-BoN BO and baseline’s generated Ad images for three fictional brands: GreenBite burger patty (Scenario 1), MindGarden meditation app (Scenario 6), and AuraSonics noise-canceling earbuds (Scenario 2). For the Ad images of the other five brand scenarios, see Figure 17 in Appendix C.

collapses the evaluation to a deterministic mapping and removes heterogeneity from personas and sampling, allowing us to test whether T-BoN BO’s performance depends on specific persona information-related setup. To ensure there is no leakage of preference, we used GPT-5 instead of Gemini 2.5 Flash for generating meta-reflection, generating textual gradients, and making Best-of-N choices.

We again compare T-BoN BO ($J=5$ trajectories) against the BEST-OF-64 initial baseline; we exclude GEPA, which requires multiple personas (multiple problems, in GEPA’s language.)

Figure 10 plots T-BoN BO across 10 optimization steps starting from the WORST5-OF-64 prompts under the ablation setup. As in Figure 8, the main experiment’s results, the value shown in Figure 10 is the mean of that step’s scores over eight scenarios. As can see in Figure 10, T-BoN BO again outperforms BEST-OF-64 baseline from optimization step 3. Except for the fact that in general the evaluation scores without persona information are more optimistic than scores with persona information for both T-BoN BO and BEST-OF-64, the ablation experiment’s trend in Figure 10 shows the same trend we saw in Figure 8.

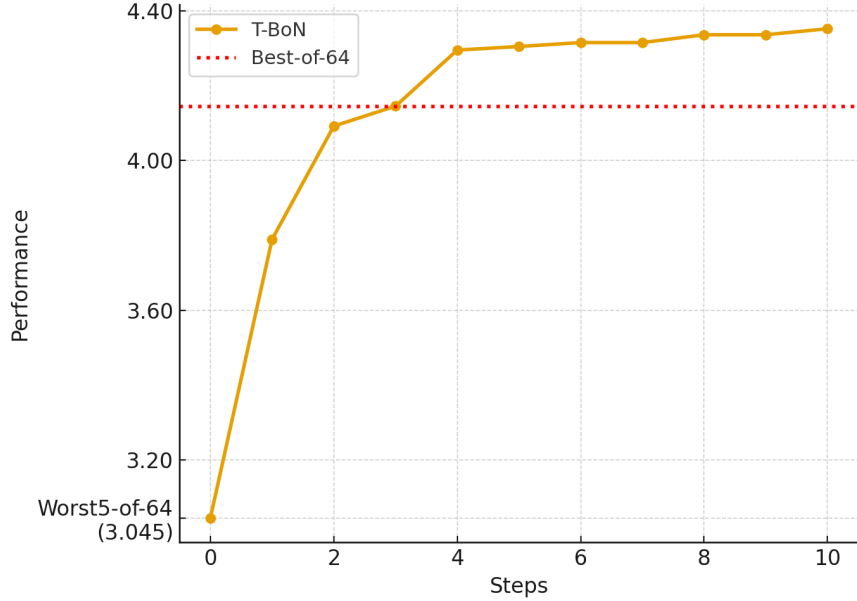


Figure 10: An ablation study experimenting T-BoN BO with $J = 5$ and BEST-OF-64 for Gemini 2.5 Flash instead of persona distribution with temperature 0. (GEPA was excluded, as there is no problem-dependent heterogeneity.) The performance score (the y -axis) is the average of eight scenarios’ mean evaluation score for the testing persona set. Again, since it is the mean of means, we don’t plot the standard deviations.

8 Conclusion

The importance of developing evaluation-efficient self-improving AI systems is substantial for its societal applications, yet this problem has remained unidentified and unaddressed. Motivated by the effectiveness of prompt optimization, which outperforms reinforcement fine-tuning methods, we formulate this problem as an iterative prompt optimization and address it.

We propose T-BoN BO, a simple, evaluation-efficient prompt optimization framework that leverages textual edits and Best-of- N search to guide prompt improvement. We prove that T-BoN BO statistically emulates UCB-BO, which is a provably evaluation-efficient algorithm. Experiments simulating ad alignment across eight creative-ad tasks demonstrate that T-BoN BO outperforms strong state-of-the-art baselines, including large BEST-OF- N and GEPA. We validate that these improvements are not attributed to the usage of specific persona dataset or trivial improvements from using poor initial prompts.

Our paper makes three key contributions to the computer science and marketing literature. First, it identifies evaluation efficiency as an essential objective for a societal self-improving system design. Second, it presents a simple yet provably efficient AI self-improving system design framework that can be applied to real-world societal systems, e.g., ad agencies, that incur high evaluation costs. Third, we theoretically prove that the presented framework is evaluation-efficient.

In sum, this work bridges classical Bayesian optimization and prompt-based self-improving AI systems, demonstrating that evaluation-efficient optimization in the prompt space is both theoretically tractable and

practically impactful. As organizations increasingly rely on AI-generated content, methods like T-BoN BO can help managers achieve higher-quality outputs without proportionally increasing evaluation burdens.

References

- Emre Can Acikgoz, Cheng Qian, Heng Ji, Dilek Hakkani-Tür, and Gokhan Tur. Self-improving llm agents at test-time. *arXiv preprint arXiv:2510.07841*, 2025.
- Virginia Aglietti, Ira Ktena, Jessica Schrouff, Eleni Sgouritsa, Francisco Ruiz, Alan Malek, Alexis Bellot, and Silvia Chiappa. Funbo: Discovering acquisition functions for bayesian optimization with funsearch. In *Forty-second International Conference on Machine Learning*, 2025.
- Lakshya A Agrawal, Shangyin Tan, Dilara Soylu, Noah Ziemis, Rishi Khare, Krista Opsahl-Ong, Arnav Singhvi, Herumb Shandilya, Michael J Ryan, Meng Jiang, et al. Gepa: Reflective prompt evolution can outperform reinforcement learning. *arXiv preprint arXiv:2507.19457*, 2025.
- Nicolás Aramayo, Mario Schiappacasse, and Marcel Goic. A multiarmed bandit approach for house ads recommendations. *Marketing Science*, 42(2):271–292, 2023.
- Wenjia Ba, J Michael Harrison, and Harikesh S Nair. Advertising media and target audience optimization via high-dimensional bandits. *arXiv preprint arXiv:2209.08403*, 2022.
- Ahmad Beirami, Alekh Agarwal, Jonathan Berant, Alexander D’Amour, Jacob Eisenstein, Chirag Nagpal, and Ananda Theertha Suresh. Theoretical guarantees on the best-of-n alignment policy. *arXiv preprint arXiv:2401.01879*, 2024.
- Tom Brown, Benjamin Mann, Nick Ryder, Melanie Subbiah, Jared D Kaplan, Prafulla Dhariwal, Arvind Neelakantan, Pranav Shyam, Girish Sastry, Amanda Askell, et al. Language models are few-shot learners. *Advances in neural information processing systems*, 33:1877–1901, 2020.
- Samuel Cahyawijaya, Holy Lovenia, and Pascale Fung. Llms are few-shot in-context low-resource language learners. *arXiv preprint arXiv:2403.16512*, 2024.
- Nitay Calderon, Roi Reichart, and Rotem Dror. The alternative annotator test for llm-as-a-judge: How to statistically justify replacing human annotators with llms. *arXiv preprint arXiv:2501.10970*, 2025.
- A Colin Cameron and Douglas L Miller. A practitioner’s guide to cluster-robust inference. *Journal of human resources*, 50(2):317–372, 2015.
- A Colin Cameron, Jonah B Gelbach, and Douglas L Miller. Robust inference with multiway clustering. *Journal of Business & Economic Statistics*, 29(2):238–249, 2011.
- Kaiyuan Chen, Yixin Ren, Yang Liu, Xiaobo Hu, Haotong Tian, Tianbao Xie, Fangfu Liu, Haoye Zhang, Hongzhang Liu, Yuan Gong, et al. xbench: Tracking agents productivity scaling with profession-aligned real-world evaluations. *arXiv preprint arXiv:2506.13651*, 2025.

Abdoulatif Cissé, Xenophon Evangelopoulos, Vladimir V Gusev, and Andrew I Cooper. Language-based bayesian optimization research assistant (bora). *arXiv preprint arXiv:2501.16224*, 2025.

Julian Coda-Forno, Marcel Binz, Zeynep Akata, Matt Botvinick, Jane Wang, and Eric Schulz. Meta-in-context learning in large language models. *Advances in Neural Information Processing Systems*, 36:65189–65201, 2023.

Patrick Coffee. Ai will soon dominate ad buying, whether marketers like it or not. *The Wall Street Journal*, March 2025. URL <https://www.wsj.com/articles/ai-will-soon-dominate-ad-buying-whether-marketers-like-it-or-not-3d62b754>.

Wendi Cui, Jiaxin Zhang, Zhuohang Li, Hao Sun, Damien Lopez, Kamalika Das, Bradley A Malin, and Sricharan Kumar. Automatic prompt optimization via heuristic search: A survey. *arXiv preprint arXiv:2502.18746*, 2025.

Li Ding, Jenny Zhang, Jeff Clune, Lee Spector, and Joel Lehman. Quality diversity through human feedback: Towards open-ended diversity-driven optimization. *arXiv preprint arXiv:2310.12103*, 2023.

Jacob Eisenstein, Chirag Nagpal, Alekh Agarwal, Ahmad Beirami, Alex D’Amour, DJ Dvijotham, Adam Fisch, Katherine Heller, Stephen Pfohl, Deepak Ramachandran, et al. Helping or herding? reward model ensembles mitigate but do not eliminate reward hacking. *arXiv preprint arXiv:2312.09244*, 2023.

Dyke Ferber, Georg Wölflein, Isabella C Wiest, Marta Ligeró, Srividhya Sainath, Narmin Ghaffari Laleh, Omar SM El Nahhas, Gustav Müller-Franzes, Dirk Jäger, Daniel Truhn, et al. In-context learning enables multimodal large language models to classify cancer pathology images. *Nature Communications*, 15(1): 10104, 2024.

Chrisantha Fernando, Dylan Banarse, Henryk Michalewski, Simon Osindero, and Tim Rocktäschel. Promptbreeder: self-referential self-improvement via prompt evolution. In *Proceedings of the 41st International Conference on Machine Learning, ICML’24*. JMLR.org, 2024.

Tanner Fiez, Houssam Nassif, Yu-Cheng Chen, Sergio Gamez, and Lalit Jain. Best of three worlds: Adaptive experimentation for digital marketing in practice. In *Proceedings of the ACM Web Conference 2024*, pages 3586–3597, 2024.

Peter I Frazier. A tutorial on bayesian optimization. *arXiv preprint arXiv:1807.02811*, 2018.

Leo Gao, John Schulman, and Jacob Hilton. Scaling laws for reward model overoptimization. In *International Conference on Machine Learning*, pages 10835–10866. PMLR, 2023.

Tong Geng, Xiliang Lin, and Harikesh S Nair. Online evaluation of audiences for targeted advertising via bandit experiments. In *Proceedings of the AAAI Conference on Artificial Intelligence*, 2020.

- Akash Ghosh, Arkadeep Acharya, Sriparna Saha, Vinija Jain, and Aman Chadha. Exploring the frontier of vision-language models: A survey of current methodologies and future directions. *arXiv preprint arXiv:2404.07214*, 2024.
- Anna Goldie, Azalia Mirhoseini, and Jeff Dean. That chip has sailed: A critique of unfounded skepticism around ai for chip design. *arXiv preprint arXiv:2411.10053*, 2024.
- Qingyan Guo, Rui Wang, Junliang Guo, Bei Li, Kaitao Song, Xu Tan, Guoqing Liu, Jiang Bian, and Yujiu Yang. Connecting large language models with evolutionary algorithms yields powerful prompt optimizers. In *The Twelfth International Conference on Learning Representations*, 2024a. URL <https://openreview.net/forum?id=ZG3RaNIso8>.
- Siyuan Guo, Cheng Deng, Ying Wen, Hechang Chen, Yi Chang, and Jun Wang. Ds-agent: Automated data science by empowering large language models with case-based reasoning. *arXiv preprint arXiv:2402.17453*, 2024b.
- Jochen Hartmann, Yannick Exner, and Samuel Domdey. The power of generative marketing: Can generative ai create superhuman visual marketing content? *International Journal of Research in Marketing*, 42(1): 13–31, 2025.
- John R Hauser, Glen L Urban, Guilherme Liberali, and Michael Braun. Website morphing. *Marketing Science*, 28(2):202–223, 2009.
- Neil He, Jiahong Liu, Buze Zhang, Ngoc Bui, Ali Maatouk, Menglin Yang, Irwin King, Melanie Weber, and Rex Ying. Position: Beyond euclidean–foundation models should embrace non-euclidean geometries. *arXiv preprint arXiv:2504.08896*, 2025.
- Kelly Hong, Anton Troynikov, and Jeff Huber. Context rot: How increasing input tokens impacts llm performance. Technical report, Chroma, July 2025. URL <https://research.trychroma.com/context-rot>.
- Xinyi Hou, Yanjie Zhao, Shenao Wang, and Haoyu Wang. Model context protocol (mcp): Landscape, security threats, and future research directions. *arXiv preprint arXiv:2503.23278*, 2025.
- Shengran Hu, Cong Lu, and Jeff Clune. Automated design of agentic systems. *arXiv preprint arXiv:2408.08435*, 2024.
- Jiaxin Huang, Shixiang Gu, Le Hou, Yuexin Wu, Xuezhi Wang, Hongkun Yu, and Jiawei Han. Large language models can self-improve. In Houda Bouamor, Juan Pino, and Kalika Bali, editors, *Proceedings of the 2023 Conference on Empirical Methods in Natural Language Processing*, pages 1051–1068, Singapore, December 2023. Association for Computational Linguistics. doi:10.18653/v1/2023.emnlp-main.67. URL <https://aclanthology.org/2023.emnlp-main.67/>.

- Tijmen Jansen, Mark Heitmann, Martin Reisenbichler, and David A Schweidel. Automated alignment: Engaging customers with visual generative ai. *Available at SSRN 4656622*, 2024.
- Yixing Jiang, Jeremy Irvin, Ji Hun Wang, Muhammad Ahmed Chaudhry, Jonathan H Chen, and Andrew Y Ng. Many-shot in-context learning in multimodal foundation models. *arXiv preprint arXiv:2405.09798*, 2024.
- Garrett A Johnson. Inferno: A guide to field experiments in online display advertising. *Journal of economics & management strategy*, 32(3):469–490, 2023.
- John Jumper, Richard Evans, Alexander Pritzel, Tim Green, Michael Figurnov, Olaf Ronneberger, Kathryn Tunyasuvunakool, Russ Bates, Augustin Židek, Anna Potapenko, et al. Highly accurate protein structure prediction with alphafold. *nature*, 596(7873):583–589, 2021.
- Omar Khattab, Arnav Singhvi, Paridhi Maheshwari, Zhiyuan Zhang, Keshav Santhanam, Sri Vardhamanan, Saiful Haq, Ashutosh Sharma, Thomas T Joshi, Hanna Moazam, et al. Dspy: Compiling declarative language model calls into self-improving pipelines. *arXiv preprint arXiv:2310.03714*, 2023.
- Ron Kohavi, Diane Tang, and Ya Xu. *Trustworthy online controlled experiments: A practical guide to a/b testing*. Cambridge University Press, 2020.
- Mingze Kong, Zhiyong Wang, Yao Shu, and Zhongxiang Dai. Meta-prompt optimization for llm-based sequential decision making, 2025. URL <https://arxiv.org/abs/2502.00728>.
- Harrison Lee, Samrat Phatale, Hassan Mansoor, Thomas Mesnard, Johan Ferret, Kellie Lu, Colton Bishop, Ethan Hall, Victor Carbune, Abhinav Rastogi, et al. Rlaif vs. rlhf: Scaling reinforcement learning from human feedback with ai feedback. *arXiv preprint arXiv:2309.00267*, 2023.
- Ang Li, Haozhe Chen, Hongseok Namkoong, and Tianyi Peng. Llm generated persona is a promise with a catch. *arXiv preprint arXiv:2503.16527*, 2025a.
- Yafu Li, Xuyang Hu, Xiaoye Qu, Linjie Li, and Yu Cheng. Test-time preference optimization: On-the-fly alignment via iterative textual feedback. *arXiv preprint arXiv:2501.12895*, 2025b.
- Aixin Liu, Bei Feng, Bing Xue, Bingxuan Wang, Bochao Wu, Chengda Lu, Chenggang Zhao, Chengqi Deng, Chenyu Zhang, Chong Ruan, et al. Deepseek-v3 technical report. *arXiv preprint arXiv:2412.19437*, 2024a.
- Fei Liu, Xialiang Tong, Mingxuan Yuan, Xi Lin, Fu Luo, Zhenkun Wang, Zhichao Lu, and Qingfu Zhang. Evolution of heuristics: Towards efficient automatic algorithm design using large language model. *arXiv preprint arXiv:2401.02051*, 2024b.
- Tennison Liu, Nicolás Astorga, Nabeel Seedat, and Mihaela van der Schaar. Large language models to enhance bayesian optimization. In *The Twelfth International Conference on Learning Representations*, 2024c.

- Yantao Liu, Zijun Yao, Rui Min, Yixin Cao, Lei Hou, and Juanzi Li. Pairjudge rm: Perform best-of-n sampling with knockout tournament, 2025. URL <https://arxiv.org/abs/2501.13007>.
- Sheng Lu, Irina Bigoulaeva, Rachneet Sachdeva, Harish Tayyar Madabushi, and Iryna Gurevych. Are emergent abilities in large language models just in-context learning? In *Proceedings of the 62nd Annual Meeting of the Association for Computational Linguistics (Volume 1: Long Papers)*, pages 5098–5139, 2024.
- Josipa Majic. Vcs wake up to vibe marketing: Ai reshaping the \$250 billion industry. *The Wall Street Journal*, 2025. URL <https://www.forbes.com/sites/josipamajic/2025/03/24/vcs-wake-up-to-vibe-marketing-ai-reshaping-the-250-billion-industry/>.
- Linda Mantia, Surojit Chatterjee, and Vivian S. Lee. Designing a successful agentic ai system. *Harvard Business Review*, 2025. URL <https://hbr.org/2025/10/designing-a-successful-agentic-ai-system>. Accessed: 2025-11-01.
- Sidharth Mudgal, Jong Lee, Harish Ganapathy, YaGuang Li, Tao Wang, Yanping Huang, Zhifeng Chen, Heng-Tze Cheng, Michael Collins, Trevor Strohman, et al. Controlled decoding from language models. *arXiv preprint arXiv:2310.17022*, 2023.
- Preetam Nandy, Divya Venugopalan, Chun Lo, and Shaunak Chatterjee. A/b testing for recommender systems in a two-sided marketplace. *Advances in Neural Information Processing Systems*, 34:6466–6477, 2021.
- Anh Nguyen, Jason Yosinski, and Jeff Clune. Understanding innovation engines: Automated creativity and improved stochastic optimization via deep learning. *Evolutionary computation*, 24(3):545–572, 2016.
- Giorgos Nikolaou, Tommaso Mencattini, Donato Crisostomi, Andrea Santilli, Yannis Panagakis, and Emanuele Rodola. Language models are injective and hence invertible. *arXiv preprint arXiv:2510.15511*, 2025.
- Siru Ouyang, Jun Yan, I Hsu, Yanfei Chen, Ke Jiang, Zifeng Wang, Rujun Han, Long T Le, Samira Daruki, Xiangru Tang, et al. Reasoningbank: Scaling agent self-evolving with reasoning memory. *arXiv preprint arXiv:2509.25140*, 2025.
- Leonard Papenmeier, Matthias Poloczek, and Luigi Nardi. Understanding high-dimensional bayesian optimization. *arXiv preprint arXiv:2502.09198*, 2025.
- Tiany Peng, George Gui, Daniel J Merlau, Grace Jiarui Fan, Malek Ben Sliman, Melanie Brucks, Eric J Johnson, Vicki Morwitz, Abdullah Althenayyan, Silvia Bellezza, et al. A mega-study of digital twins reveals strengths, weaknesses and opportunities for further improvement. *arXiv preprint arXiv:2509.19088*, 2025.
- Jiahao Qiu, Xuan Qi, Hongru Wang, Xinzhe Juan, Yimin Wang, Zelin Zhao, Jiayi Geng, Jiacheng Guo, Peihang Li, Jingzhe Shi, et al. Alita-g: Self-evolving generative agent for agent generation. *arXiv preprint arXiv:2510.23601*, 2025.

- Nils Reimers and Iryna Gurevych. Sentence-bert: Sentence embeddings using siamese bert-networks. *arXiv preprint arXiv:1908.10084*, 2019.
- Daniel Russo. Simple bayesian algorithms for best arm identification. In *Conference on learning theory*, pages 1417–1418. PMLR, 2016.
- Jonathan Scarlett, Ilija Bogunovic, and Volkan Cevher. Lower bounds on regret for noisy gaussian process bandit optimization. In *Conference on Learning Theory*, pages 1723–1742. PMLR, 2017.
- Lennart Schneider, Martin Wistuba, Aaron Klein, Jacek Golebiowski, Giovanni Zappella, and Felice Antonio Merra. Hyperband-based bayesian optimization for black-box prompt selection. In *Forty-second International Conference on Machine Learning*, 2025. URL <https://openreview.net/forum?id=Lm9DXFrCHD>.
- Eric M Schwartz, Eric T Bradlow, and Peter S Fader. Customer acquisition via display advertising using multi-armed bandit experiments. *Marketing Science*, 36(4):500–522, 2017.
- Lin Shi, Chiyu Ma, Wenhua Liang, Weicheng Ma, and Soroush Vosoughi. Judging the judges: A systematic investigation of position bias in pairwise comparative assessments by llms. *arXiv*, 2024. URL <https://arxiv.org/abs/2406.07791>. arXiv:2406.07791 [cs.CL].
- David Silver and Richard S Sutton. Welcome to the era of experience. *Google AI*, 1, 2025.
- Joykirat Singh, Subhabrata Dutta, and Tanmoy Chakraborty. Mechanistic behavior editing of language models, 2025.
- Charlie Snell, Jaehoon Lee, Kelvin Xu, and Aviral Kumar. Scaling llm test-time compute optimally can be more effective than scaling model parameters. *arXiv preprint arXiv:2408.03314*, 2024.
- Dilara Soylu, Christopher Potts, and Omar Khattab. Fine-tuning and prompt optimization: Two great steps that work better together, 2024. URL <https://arxiv.org/abs/2407.10930>.
- Niranjan Srinivas, Andreas Krause, Sham M Kakade, and Matthias W Seeger. Information-theoretic regret bounds for gaussian process optimization in the bandit setting. *IEEE transactions on information theory*, 58(5):3250–3265, 2012.
- Eric Tang, Bangding Yang, and Xingyou Song. Understanding LLM embeddings for regression. *Transactions on Machine Learning Research*, 2025. ISSN 2835-8856. URL <https://openreview.net/forum?id=Wt6Iz5XNIO>.
- Olivier Toubia, George Z Gui, Tianyi Peng, Daniel J Merlau, Ang Li, and Haozhe Chen. Twin-2k-500: A dataset for building digital twins of over 2,000 people based on their answers to over 500 questions. *arXiv preprint arXiv:2505.17479*, 2025.

- Roman Vershynin. *High-dimensional probability: An introduction with applications in data science*, volume 47. Cambridge university press, 2018.
- Tomoya Wakayama and Taiji Suzuki. In-context learning is provably bayesian inference: a generalization theory for meta-learning. *arXiv preprint arXiv:2510.10981*, 2025.
- Wenjia Wang, Xiaowei Zhang, and Lu Zou. Regret optimality of gp-ucb. *arXiv preprint arXiv:2312.01386*, 2023a.
- Wenxiao Wang, Priyatham Kattakinda, and Soheil Feizi. Maestro: Joint graph & config optimization for reliable ai agents. *arXiv preprint arXiv:2509.04642*, 2025.
- Xinyi Wang, Wanrong Zhu, Michael Saxon, Mark Steyvers, and William Yang Wang. Large language models are latent variable models: Explaining and finding good demonstrations for in-context learning. *Advances in Neural Information Processing Systems*, 36:15614–15638, 2023b.
- Justin Whitehouse, Aaditya Ramdas, and Steven Z Wu. On the sublinear regret of gp-ucb. *Advances in Neural Information Processing Systems*, 36:35266–35276, 2023.
- Thaddäus Wiedemer, Yuxuan Li, Paul Vicol, Shixiang Shane Gu, Nick Matarese, Kevin Swersky, Been Kim, Priyank Jaini, and Robert Geirhos. Video models are zero-shot learners and reasoners, 2025. URL <https://arxiv.org/abs/2509.20328>.
- James Wilson, Frank Hutter, and Marc Deisenroth. Maximizing acquisition functions for bayesian optimization. *Advances in neural information processing systems*, 31, 2018.
- Sang Michael Xie, Aditi Raghunathan, Percy Liang, and Tengyu Ma. An explanation of in-context learning as implicit bayesian inference. *arXiv preprint arXiv:2111.02080*, 2021.
- Chengrun Yang, Xuezhi Wang, Yifeng Lu, Hanxiao Liu, Quoc V. Le, Denny Zhou, and Xinyun Chen. Large language models as optimizers, 2024. URL <https://arxiv.org/abs/2309.03409>.
- Nicholas Young. *An introduction to Hilbert space*. Cambridge university press, 1988.
- Mert Yuksekogonul, Federico Bianchi, Joseph Boen, Sheng Liu, Pan Lu, Zhi Huang, Carlos Guestrin, and James Zou. Optimizing generative ai by backpropagating language model feedback. *Nature*, 639:609–616, 2025.
- Qizheng Zhang, Changran Hu, Shubhangi Upasani, Boyuan Ma, Fenglu Hong, Vamsidhar Kamanuru, Jay Rainton, Chen Wu, Mengmeng Ji, Hanchen Li, et al. Agentic context engineering: Evolving contexts for self-improving language models. *arXiv preprint arXiv:2510.04618*, 2025.
- Yongchao Zhou, Andrei Ioan Muresanu, Ziwen Han, Keiran Paster, Silviu Pitis, Harris Chan, and Jimmy Ba. Large language models are human-level prompt engineers. In *The eleventh international conference on learning representations*, 2022.

A Prompts used for digital marketing

Best-of-N Gradient steps' pairwise tournament prompt for ads.

```
contents = [image1, image2, comparison_prompt]
comparison_prompt =
    "You are evaluating two advertisement images for mobile Instagram ads. Which image would be more effective at engaging users and driving clicks?
    RESPOND WITH ONLY THE NUMBER 1 OR 2. NOTHING ELSE.
    1 = first image is better
    2 = second image is better "
```

Figure 11: M_{critic} 's pairwise tournament prompt for digital marketing example.

Meta reflection prompt for ads

You are an expert at analyzing visual patterns in advertising performance.

VISUAL ANALYSIS TASK:

I will show you images from the lowest-scoring and highest-scoring ad iterations. Your task is to identify specific visual patterns that distinguish effective from ineffective ads.

VISUAL EXAMPLES – BEST VS WORST PERFORMING:

RANK 1/10 WORST PERFORMING (Score: 2.14/5.0):

Prompt excerpt: <prompt>...

[Image]

RANK 2/10 LOWER HALF (Score: 2.52/5.0):

Prompt excerpt: <prompt>...

[Image]

...

RANK 9/10 UPPER HALF (Score: 3.81/5.0):

Prompt excerpt: <prompt>...

[Image]

RANK 10/10 BEST PERFORMING (Score: 4.15/5.0):

Prompt excerpt: <prompt>...

[Image]

Based on your visual analysis, identify patterns that correlate with higher effectiveness scores:

1. Visual composition and framing differences
2. Lighting conditions and mood variations
3. Color palettes and visual tone patterns
4. Subject positioning and action effectiveness
5. Brand integration approaches
6. Environmental and atmospheric elements

RESPONSE FORMAT:

Provide a structured analysis of visual patterns observed, focusing on what distinguishes high-performing from low-performing ads.

Figure 12: Meta reflection prompt for digital marketing example.

Prompt used for generating prompts for ads generation

Generate a creative, structured and descriptive prompt for a generative AI model (e.g., Imagen) that will produce a brand-aligned, and scroll-stopping advertisement image suitable for an Instagram feed.

A successful prompt must be constructed using the following components and principles:

0. (Most important!) Prompt NEVER includes any description of kids. Kids are not allowed to generate in Imagen 4. Even if creative_brief includes description of "family" or "kids", never include kids in the prompt. Only create adults if humans are included.

1. Key Message (The "Why"): This is the foundational element that guides all other components. It defines the core idea or feeling the ad must communicate. Before writing the rest of the prompt, clearly articulate the message the ad will deliver. This message will act as the "North Star" for all subsequent creative choices. It may be desirable to put the message as the text overlay.

2. Core Components (The "What"):

- This should completely depend on the key message.
- Scene & Environment: Based on the key message, establish a clear, relatable setting that aligns with the brand's lifestyle appeal.
- Action & Narrative: Based on the key message and the scene, describe a dynamic but clear action or interaction to create a sense of a captured moment and tell a micro-story.
- Composition & Framing: Specify the camera shot, angle, and framing (e.g., "low-angle shot," "dynamic medium shot," "close-up on the shoe").

3. Stylistic Qualities (The "How"):

- This should completely depend on the key message and the scene.
- Photography Style: Define the overall aesthetic (e.g., "photorealistic," "cinematic," "professional product photography," "lifestyle action shot").
- Lighting: Be specific about the lighting to set the mood (e.g., "warm golden hour light," "bright morning sun," "dramatic side-lighting").
- Color Palette & Tone: Guide the color scheme and emotional feel (e.g., "vibrant and energetic colors," "empowering and motivational tones," "clean and modern palette").
- Atmosphere & Feeling: Aim to evoke a specific feeling aligned with the brand (e.g., "a feeling of effortless performance," "an atmosphere of vibrant energy," "a sense of supreme comfort").

4. What to Avoid:

- Vagueness: Use specific, descriptive terms instead of "nice" or "good."
- Contradictory Elements: Ensure all elements work together harmoniously.
- Over-stuffing: Focus on a single, clear message without too many competing objects.

5. What to include:

- Logo: create a logo based on creative brief, and naturally place it.
- Text: If you are including a text message, prompt for "negative space for text overlay".

Figure 13: Prompt for generating the prompts for the initial 64 ads.

Prompt for generating the worst-of-64 in GreenBite (plant-based burger patty) ad scenario.

****Key Message:**** To visually communicate the core idea: "Experience the juicy, no-compromise satisfaction of a real burger, made better for you and the planet."

****Image Generation Prompt:**** A dynamic, commercial lifestyle photograph for an Instagram feed ad.

****Core Components:****

- **Scene & Environment:**** A stylish, modern outdoor patio during a late afternoon barbecue. The background is softly blurred, showing contemporary patio furniture, lush green potted plants, and the warm glow of string lights just beginning to turn on.
- **Subject & Action:**** The focal point is a vibrant, stylish woman in her early thirties, captured in a candid moment of pure satisfaction. She is taking a bite of a huge, delicious-looking plant-based burger. Her eyes are closed in bliss, and a small, genuine smile plays on her lips, conveying an authentic "this is amazing" reaction. Juice from the burger is subtly visible on her hand to emphasize its succulence. She is dressed in a casual but chic linen shirt.
- **Product:**** The GreenBite burger is the hero. It's a thick, perfectly seared patty with grill marks, nestled in a glossy brioche bun. It's layered with glistening melted cheddar cheese, crisp green lettuce, a thick slice of ripe red tomato, and caramelized onions spilling out slightly. The burger is partially wrapped in a simple, brown kraft paper sheet which has a small, clean logo on it: "GreenBite" in a modern sans-serif font next to a stylized green leaf.
- **Composition & Framing:**** A medium close-up shot, angled slightly upwards to make the moment feel triumphant and empowering. The camera uses a shallow depth of field, keeping the woman's expression and the burger in sharp focus while the background is beautifully out of focus (bokeh). The composition is balanced, with a clear area of soft background on the upper right side, creating negative space for a text overlay.
- **Stylistic Qualities:****
- **Photography Style:**** High-end, photorealistic commercial food photography with a warm, authentic lifestyle feel. The image should be incredibly sharp and detailed, especially the texture of the burger patty and the fresh ingredients.
- **Lighting:**** Bathed in the warm, dreamy glow of the golden hour. The sunlight comes from the side, creating soft highlights and long, gentle shadows, emphasizing the textures of the food and giving her skin a radiant look.
- **Color Palette & Tone:**** A rich and mouth-watering color palette. Saturated and vibrant, but natural. Warm tones of orange, gold, and red from the sun and the food are balanced by the deep greens of the background foliage and the crispness of the lettuce.
- **Atmosphere & Feeling:**** The image radiates a feeling of guilt-free indulgence, vibrant well-being, and ultimate satisfaction. The atmosphere is confident, positive, and irresistibly appetizing, making the viewer crave that exact experience.

Prompt for generating the best-of-64 in GreenBite (plant-based burger patty) ad scenario.

****1. Key Message (The "Why"):** To visually capture the peak moment of guilt-free indulgence, proving that a plant-based burger can deliver an unbelievably juicy, satisfying, and no-compromise flavor experience identical to a classic beef burger. The text overlay will read: "The No-Compromise Burger."

****2. Core Components (The "What"):**

- **Scene & Environment:**** A vibrant, sun-drenched backyard barbecue scene, shot with a very shallow depth of field. The background is a beautiful, soft-focus bokeh of friends laughing (adults only, 25-40 age range), string lights, and lush greenery, suggesting a warm, sociable atmosphere without distracting from the main subject.
- **Action & Narrative:**** A stylish woman in her early 30s, with a look of pure, blissful satisfaction, is taking the first, epic bite of a burger. Her eyes are closed in enjoyment. Her hands grip the burger firmly but gently. A single, perfect drop of sauce is starting to fall from the side of the burger, caught in mid-air, emphasizing its juiciness.
- **Composition & Framing:**** A dramatic, macro close-up, food photography style. The shot is framed tightly on the lower half of the woman's face and her hands holding the burger, making the burger the undeniable hero. The angle is slightly low to give the burger an epic, monumental feel. The right side of the frame has clean, out-of-focus background elements, creating intentional negative space for a text overlay.

****3. Stylistic Qualities (The "How"):**

- **Photography Style:**** Hyper-realistic, professional commercial food photography. Every detail is rendered with extreme clarity: the char marks on the patty, the condensation on the lettuce, the glistening melt of the plant-based cheese, and the texture of the toasted brioche bun. Shot with a high-end DSLR camera and a macro lens.
- **Lighting:**** Warm, radiant golden hour lighting. The sun acts as a dramatic backlight, creating a halo effect around the burger and the woman's hands, and creating glistening specular highlights on the juicy patty and sauce. The lighting is bright, positive, and makes the food look incredibly appetizing.
- **Color Palette & Tone:**** A mouth-watering and vibrant palette. Rich, savory browns of the seared "GreenBite" patty, deep reds of a ripe tomato slice, vibrant green of crisp lettuce, and a warm golden-yellow of the melted cheese and toasted bun. The overall tone is confident, delicious, and energetic.
- **Atmosphere & Feeling:**** The atmosphere is one of ultimate satisfaction and pure, unadulterated foodie bliss. It feels warm, authentic, and completely satisfying, eliminating any doubt about the quality and taste of the plant-based option.

****4. Inclusions & Details:**

- **The Burger Details:**** The GreenBite patty is thick, with a perfect, glistening sear and visible char marks, looking indistinguishable from high-quality ground beef. It's topped with melting vegan cheddar cheese, a leaf of crisp butter lettuce, a thick slice of heirloom tomato, and a creamy aioli sauce.
- **Logo Placement:**** The burger is partially wrapped at the base with a small square of branded, unbleached butcher paper. The "GreenBite" logo—a simple, modern green leaf icon next to the word "GreenBite" in a clean sans-serif font—is subtly visible on the paper.
- **Negative Space:**** Ensure the composition leaves a clean, uncluttered area of soft-focus background on the right third of the image for text overlay.

Figure 14: Prompts for the best and worst ad among the initial 64 ads.

Prompt for generating the T-BoN ($T = 10$) ad for GreenBite (plant-based burger patty)

***Key Message:**

"The No-Compromise Burger"—to visually prove that a plant-based burger can be just as juicy, delicious, and satisfying as a traditional beef burger, making it the hero of the ultimate backyard BBQ.

*Core Components:**

***Scene & Environment:** A vibrant, meticulously designed modern backyard patio, perfect for a relaxed, aspirational late-afternoon get-together. The background is a soft-focus composition of stylish outdoor furniture, lush green garden plants, and subtly visible, engaged friends enjoying themselves and partaking in the shared experience. Occasional hints of other complementary gourmet side dishes or refreshing beverages on the blurred patio table enhance the sense of a complete, desirable BBQ experience, creating a rich, warm, and inviting social atmosphere.

***Action & Narrative:** A pair of adult hands are holding up a perfectly constructed, gourmet-style cheeseburger. The action captures either: (A) a moment of serene, authentic anticipation just before the first bite, with the subject's face (in soft focus) conveying genuine contentment or subtle bliss, possibly with eyes gently closed, savoring the aroma; OR (B) the burger held out slightly towards the camera, inviting the viewer into the experience, with the subject's soft-focus expression conveying a shared, authentic delight or playful 'aha!' moment. The emphasis is on genuine human emotion and connection, avoiding any forced, exaggerated, or unnatural expressions (especially if a bite is implied). A single, glistening drop of rich, savory juice is visible, about to fall from the patty, powerfully emphasizing its irresistible succulence and indulgent quality without appearing messy. ***Central Subject:** The star of the image is the GreenBite burger. It's a thick, plant-based patty with a deeply browned, flawlessly seared crust and visible grill marks, looking indistinguishable from premium ground beef. It's topped with a layer of glistening, perfectly melted cheddar cheese, a crisp piece of bright green leaf lettuce, a thick, ruby-red slice of a heirloom tomato, and a few rings of sharp red onion, all between a fluffy, toasted brioche bun. ***Composition & Framing:** An enticing, slightly low-angle medium close-up shot where the GreenBite burger is the undeniable hero, prominently filling a significant portion of the frame and drawing the viewer's eye directly to its appetizing qualities. The focus is tack-sharp on the GreenBite patty's seared texture and the glistening juice. The hands holding the burger, and the subject's face (if present), along with the backyard scene, are rendered in a beautiful, soft-focus bokeh, creating a strong emotional connection and aspirational appeal while ensuring the burger remains supremely appetizing. There is significant negative space with soft, blurred greenery in the upper portion of the frame for a text overlay.

Stylistic Qualities:

***Photography Style:** High-end, photorealistic commercial food photography with a cinematic lifestyle feel. The image should be incredibly crisp, detailed, and textured. ***Lighting:** Bathed in the warm, dreamy glow of golden hour sunlight. The light source comes from the side, casting soft shadows that accentuate the burger's shape and highlight the glistening textures of the melted cheese and juicy patty. A slight, elegant lens flare bleeds into the frame, adding to the warm, aspirational feel. ***Color Palette & Tone:** Rich, saturated, and mouth-watering. A color palette dominated by the warm browns of the seared patty, the vibrant orange of the cheese, the fresh greens of the lettuce, and the deep reds of the tomato, all set against the warm, earthy tones of the background.

***Atmosphere & Feeling:** Evokes a powerful feeling of shared satisfaction, vibrant well-being, and guilt-free indulgence. The atmosphere is confidently positive, supremely delicious, and distinctly aspirational, conveying a desirable lifestyle of effortless enjoyment. **Brand Elements:**

Logo: The simple, modern "GreenBite" logo (clean sans-serif font with a subtle leaf element) is integrated prominently yet naturally within the scene. It is elegantly printed on the branded wax paper partially wrapping the bottom of the burger, and also subtly visible on a branded napkin or a stylish sauce bottle on the blurred patio table in the background, reinforcing brand presence contextually within the aspirational setting. * In addition to the physical logo placements, a clean, prominent text overlay of the 'GreenBite' brand name, and optionally a relevant tagline (e.g., 'Believe Your Bite'), should be integrated into the significant negative space in the upper portion of the frame. This overlay should be highly legible and reinforce clear brand recognition without detracting from the visual appeal."

Figure 15: Prompts for T-BoN ($T = 10$)

Prompt for generating the GEPA ($T = 10$) ad for GreenBite (plant-based burger patty)

*****Key Message:****

Visually communicate the "no-compromise" promise of GreenBite by capturing the exact moment of pure, blissful satisfaction of a consumer realizing a plant-based burger can be just as juicy and delicious as its beef counterpart.

****Core Components:****

* **Scene & Environment:** A vibrant, sun-drenched modern backyard patio during a relaxed get-together of friends in their late 20s and early 30s. The setting is stylish and aspirational, featuring a natural wood deck, comfortable outdoor furniture, festoon string lights, and lush, green potted plants in the background.

* **Action & Narrative:** The central focus is a woman with her eyes open, full of genuine, surprised satisfaction, capturing the peak moment of consumption. Her mouth is wide open, actively biting into the fully-loaded GreenBite burger. The patty is clearly visible within her mouth, emphasizing the powerful 'A-ha!' moment of discovery and the sheer indulgence of the bite, directly communicating the 'no-compromise' promise.

* **Composition & Framing:** Dynamic, slightly low-angle medium shot focusing on the woman and the burger. The burger is the hero; the depth of field is shallow, rendering the juicy, perfectly seared patty, melted plant-based cheddar, crisp lettuce, and glossy brioche bun in hyper-detailed, sharp focus. The background is beautifully out of focus with a pleasing bokeh effect. There is negative space in the upper left corner suitable for a text overlay.

* **Stylistic Qualities:** * **Photography Style:** High-end, commercial lifestyle food photography. Polished, authentic, and incredibly photorealistic. Looks like an image from a top-tier food publication. * **Lighting:** Bathed in warm, cinematic golden hour sunlight. The light creates long, soft shadows and a beautiful, inviting glow, highlighting the textures of the food. Crucially, integrate a strong, warm sun flare or haze into the scene, creating a dramatic, aspirational glow that enhances the sense of satisfaction and makes the overall atmosphere feel more vibrant and special. * **Color Palette & Tone:** Rich, warm, and saturated colors. Deep browns of the seared patty, vibrant greens of the lettuce and surrounding plants, warm yellows and oranges from the cheese and sunlight. The overall tone is confident, energetic, and mouth-watering.

* **Atmosphere & Feeling:** A powerful feeling of guilt-free indulgence and vibrant satisfaction. The atmosphere is warm, happy, and effortlessly cool, capturing the joy of sharing great food with friends. * **Inclusions:**

* **Logo:** Ensure the 'GreenBite' logo is subtly yet clearly visible on the burger wrapper, or on a small, non-distracting element within the scene, to provide product context without pulling focus from the main action.

* **Text Overlay:** A prominent, clean white text overlay, featuring a strong, benefit-driven headline such as 'THE NO-COMPROMISE BURGER' or 'BEYOND EXPECTATION.', is strategically placed in the negative space (e.g., upper left corner). This headline should be clearly legible, visually impactful, and act as a primary visual element, prioritizing the core message and value proposition over just generic brand reinforcement."

Figure 16: Prompts for GEPA ($T = 10$)

B Scenarios

Below are ten ad campaign scenarios with creative briefs, outlining the strategic and creative direction for each experimental scenario. The selected campaigns cover a diverse range of products across distinct categories. Each campaign addresses a unique consumer need—whether related to sustainability, luxury, technology, or lifestyle—ensuring comprehensive coverage of various market segments. From environmentally-conscious millennials to affluent, experience-driven travelers, the approach accounts for the full spectrum of consumer interests. By focusing on different consumer needs, the structure enables a holistic marketing strategy that captures both niche and broad demands, providing a well-rounded framework for the study.

B.1 Scenario 1: GreenBite Plant-Based Burger

- **Product:** "GreenBite," a new plant-based burger patty.
- **Background:** The market for plant-based food is growing, but many consumers remain skeptical about taste, believing they must sacrifice flavor for health.
- **The Challenge:** Convince flexitarians that GreenBite offers the juicy, satisfying experience of a traditional beef burger with no compromise.
- **Core Insight:** Consumers want to eat better for themselves and the planet, but they fear it means giving up the foods they love.
- **Single-Minded Proposition (SMP):** The delicious, no-compromise burger experience that's better for you and the planet.
- **Reasons to Believe (RTB):** Made with savory pea protein; sears and tastes like real beef; free of soy and GMOs.
- **Desired Response: Think:** "I can finally have a plant-based burger that tastes like the real thing.", **Feel:** Satisfied, vibrant, and guilt-free. **Do:** Purchase GreenBite for their next barbecue.
- **Brand Personality & Tone:** Positive, confident, and mouth-watering.

B.2 Scenario 2: AuraSonics X1 Earbuds

- **Product:** "AuraSonics X1," high-end, noise-canceling wireless earbuds.
- **Background:** The rise of hybrid work and urban density has increased daily auditory overload, making focus a precious commodity.
- **The Challenge:** Cut through the saturated audio market by positioning the X1 not as a gadget, but as an essential tool for mental clarity.
- **Core Insight:** In a world of constant noise, true luxury is the ability to control your own soundscape.

- **Single-Minded Proposition (SMP):** AuraSonics X1 creates a personal sanctuary for focus and immersion.
- **Reasons to Believe (RTB):** Adaptive Active Noise Cancellation; studio-quality audio; all-day battery life; minimalist aluminum design.
- **Desired Response: Think:** "This is the solution I need to escape the daily chaos." **Feel:** Calm, empowered, and sophisticated. **Do:** Visit the website to learn more.
- **Brand Personality & Tone:** Minimalist, intelligent, and calm.

B.3 Scenario 3: Odyssey E-SUV

- **Product:** The "Odyssey E-SUV," a new all-electric family SUV.
- **Background:** Many families want to switch to electric vehicles but are concerned about sacrificing space, safety, and range for sustainability.
- **The Challenge:** Position the Odyssey E-SUV as the first EV that meets all the practical and adventurous needs of a modern family, making the switch to electric feel like an upgrade, not a compromise.
- **Single-Minded Proposition (SMP):** The future of family adventure is here: all-electric, zero compromise.
- **Reasons to Believe (RTB):** 500km range; top-tier safety rating; spacious three-row seating; all-wheel drive capability.
- **Desired Response: Think:** "An electric car can actually handle my family's active lifestyle." **Feel:** Adventurous, optimistic, and secure. **Do:** Schedule a test drive.
- **Brand Personality & Tone:** Inspiring, capable, and forward-thinking.

B.4 Scenario 4: Oasis Eco-Lodge

- **Product:** "Oasis Eco-Lodge," a secluded, luxury resort operating in harmony with its natural surroundings.
- **Background:** The luxury travel market often equates opulence with excess. A growing segment of affluent travelers seeks experiences that are both exclusive and responsible.
- **The Challenge:** Redefine luxury as a seamless integration with nature, promising an experience that is restorative for both the guest and the environment.
- **Core Insight:** For those who have everything, true luxury is not more things, but a deeper connection to something pure and serene.

- **Single-Minded Proposition (SMP):** Rediscover tranquility in a luxury that respects nature.
- **Reasons to Believe (RTB):** Secluded private bungalows; farm-to-table dining with locally sourced ingredients; carbon-neutral operations.
- **Desired Response: Think:** "This is a truly special escape, not just another five-star hotel." **Feel:** Serene, exclusive, and rejuvenated. **Do:** Book a stay.
- **Brand Personality & Tone:** Elegant, peaceful, and understated.

B.5 Scenario 5: Momentum Digital Banking

- **Product:** "Momentum," a mobile-first banking app for freelancers and the gig economy.
- **Background:** Traditional banks are not built for the fluctuating incomes and unique business needs of self-employed professionals.
- **The Challenge:** Position Momentum as the essential financial co-pilot for the independent worker, simplifying complexity and providing stability.
- **Core Insight:** Freelancers love their freedom but feel anxious about their financial instability. They need a tool that brings order to their financial chaos.
- **Single-Minded Proposition (SMP):** Banking that is as flexible and entrepreneurial as you are.
- **Reasons to Believe (RTB):** Automated tax-saving tools; integrated invoicing and payment tracking; instant business expense categorization.
- **Desired Response: Think:** "Finally, a bank that gets the way I work." **Feel:** Empowered, organized, and financially confident. **Do:** Download the app and open an account.
- **Brand Personality & Tone:** Modern, empowering, and simple.

B.6 Scenario 6: MindGarden Meditation App

- **Product:** "MindGarden," a subscription-based meditation and mindfulness app.
- **Background:** While many are interested in mindfulness for stress-relief, they are often intimidated by the practice, seeing it as difficult or time-consuming.
- **The Challenge:** Make meditation feel accessible and achievable for absolute beginners, removing the barriers of time and perceived difficulty.
- **Core Insight:** People want the benefits of mindfulness but are convinced they don't have the time or ability to practice it correctly.

- **Single-Minded Proposition (SMP):** Find your calm in just 5 minutes a day.
- **Reasons to Believe (RTB):** Guided 5-minute sessions for specific needs (anxiety, focus); progress tracking to build a habit; simple, jargon-free instructions.
- **Desired Response: Think:** "I can do this. 5 minutes is easy." **Feel:** Calm, supported, and hopeful. **Do:** Start a free trial.
- **Brand Personality & Tone:** Gentle, approachable, and encouraging.

B.7 Scenario 7: Aeterno Watch

- **Product:** The "Aeterno," a classic, automatic Swiss-made wristwatch with a heritage design.
- **Background:** In an age of smartwatches that are obsolete in a few years, there is a renewed appreciation for objects with permanence and enduring value.
- **The Challenge:** Reassert the relevance of the classic mechanical watch as a symbol of taste, craftsmanship, and timelessness.
- **Core Insight:** In a disposable world, true status comes from owning something permanent that tells a story.
- **Single-Minded Proposition (SMP):** A legacy on your wrist. Craftsmanship that transcends time.
- **Reasons to Believe (RTB):** Swiss-made automatic movement; sapphire crystal glass; timeless design inspired by 1950s classics.
- **Desired Response: Think:** "This is a beautiful object that I will own forever." **Feel:** Prestigious, sophisticated, and discerning. **Do:** Locate an authorized dealer.
- **Brand Personality & Tone:** Elegant, timeless, and confident.

B.8 Scenario 8: SyncFlow B2B Software

- **Product:** "SyncFlow," a project management and collaboration software platform for remote teams.
- **Background:** Remote work has increased flexibility but also created challenges in team alignment, communication, and project visibility.
- **The Challenge:** Cut through a crowded SaaS market by focusing on the outcome of "effortless collaboration" rather than just listing features.
- **Core Insight:** Managers don't want another tool to manage; they want the feeling of clarity and momentum that comes from a team working in perfect sync.

- **Single-Minded Proposition (SMP):** Bring your remote team together for effortless collaboration and remarkable results.
- **Reasons to Believe (RTB):** Centralized dashboards with real-time project status; integrated communication channels; automated workflows and reporting.
- **Desired Response: Think:** "This could finally solve our remote work chaos and get everyone on the same page." **Feel:** Organized, in control, and successful. **Do:** Sign up for a team demo.
- **Brand Personality & Tone:** Professional, efficient, and innovative.

C Extended experiment results

T-BoN BO										
	Aeterno	Aurasonics	Greenbite	Mindgarden	Momentum	Oasis	Odyssey	Syncflow	Average	
Worst5-of-N	2.942 (0.025)	2.793 (0.023)	2.706 (0.024)	2.722 (0.024)	2.644 (0.024)	2.839 (0.025)	2.828 (0.025)	2.641 (0.023)	2.739	
Steps	1	3.098 (0.028)	2.813 (0.022)	3.001 (0.027)	2.980 (0.027)	2.799 (0.027)	3.062 (0.028)	2.943 (0.027)	2.927 (0.023)	2.932
	2	3.125 (0.026)	2.969 (0.027)	3.041 (0.026)	2.980 (0.027)	2.907 (0.025)	3.107 (0.026)	2.943 (0.027)	2.927 (0.023)	2.982
	3	3.125 (0.026)	3.041 (0.025)	3.041 (0.026)	2.980 (0.027)	2.907 (0.025)	3.131 (0.019)	3.063 (0.019)	2.927 (0.023)	3.013
	4	3.194 (0.029)	3.041 (0.025)	3.041 (0.026)	3.132 (0.022)	2.907 (0.025)	3.324 (0.028)	3.063 (0.019)	2.927 (0.023)	3.062
	5	3.194 (0.029)	3.041 (0.025)	3.076 (0.026)	3.132 (0.022)	2.907 (0.025)	3.324 (0.028)	3.063 (0.019)	3.127 (0.022)	3.096
	6	3.257 (0.023)	3.041 (0.025)	3.076 (0.026)	3.132 (0.022)	2.907 (0.025)	3.324 (0.028)	3.070 (0.022)	3.127 (0.022)	3.097
	7	3.257 (0.023)	3.104 (0.028)	3.076 (0.026)	3.132 (0.022)	2.907 (0.025)	3.324 (0.028)	3.107 (0.027)	3.127 (0.022)	3.111
	8	3.257 (0.023)	3.104 (0.028)	3.076 (0.026)	3.132 (0.022)	2.913 (0.026)	3.324 (0.028)	3.107 (0.027)	3.127 (0.022)	3.112
	9	3.257 (0.023)	3.104 (0.028)	3.076 (0.026)	3.132 (0.022)	2.926 (0.026)	3.324 (0.028)	3.107 (0.027)	3.127 (0.022)	3.114
	10	3.257 (0.023)	3.104 (0.028)	3.168 (0.025)	3.132 (0.022)	3.024 (0.025)	3.324 (0.028)	3.107 (0.027)	3.127 (0.022)	3.155
Best-of-N	2.982 (0.025)	2.934 (0.027)	2.898 (0.025)	2.930 (0.028)	3.030 (0.027)	3.265 (0.022)	2.966 (0.027)	3.086 (0.023)	3.011	

Table 2: Progress of T-BoN BO across 10 optimization steps from its starting point (Worst5-of-N) and comparison with the BEST-of-N baseline. Each data point, in the mean (standard error) format, indicates the mean and standard error across 411 personas in the test persona set. The last column, labeled “Average”, reports the averages of the means across the eight scenarios.

GEPA										
	Aeterno	Aurasonics	Greenbite	Mindgarden	Momentum	Oasis	Odyssey	Syncflow	Average	
Worst5-of-N	2.942 (0.025)	2.793 (0.023)	2.706 (0.024)	2.722 (0.024)	2.644 (0.024)	2.839 (0.025)	2.828 (0.025)	2.641 (0.023)	2.739	
Steps	1	3.036 (0.025)	2.942 (0.025)	3.029 (0.025)	2.841 (0.024)	2.816 (0.024)	3.151 (0.024)	2.915 (0.025)	2.880 (0.025)	2.939
	2	3.036 (0.025)	2.942 (0.025)	3.046 (0.024)	2.945 (0.023)	2.907 (0.023)	3.151 (0.024)	3.071 (0.028)	2.880 (0.025)	2.992
	3	3.036 (0.025)	2.942 (0.025)	3.046 (0.024)	2.945 (0.023)	2.907 (0.023)	3.182 (0.025)	3.088 (0.026)	2.914 (0.018)	3.003
	4	3.138 (0.025)	3.028 (0.022)	3.046 (0.024)	2.954 (0.024)	2.976 (0.026)	3.187 (0.023)	3.088 (0.026)	2.949 (0.028)	3.033
	5	3.138 (0.025)	3.028 (0.022)	3.046 (0.024)	3.012 (0.022)	2.976 (0.026)	3.187 (0.023)	3.088 (0.026)	3.008 (0.026)	3.049
	6	3.157 (0.023)	3.028 (0.022)	3.046 (0.024)	3.012 (0.022)	2.976 (0.026)	3.209 (0.020)	3.088 (0.026)	3.008 (0.026)	3.052
	7	3.157 (0.023)	3.028 (0.022)	3.046 (0.024)	3.068 (0.027)	2.976 (0.026)	3.209 (0.020)	3.088 (0.026)	3.008 (0.026)	3.060
	8	3.157 (0.023)	3.028 (0.022)	3.046 (0.024)	3.068 (0.027)	2.976 (0.026)	3.209 (0.020)	3.088 (0.026)	3.008 (0.026)	3.060
	9	3.157 (0.023)	3.028 (0.022)	3.046 (0.024)	3.068 (0.027)	2.976 (0.026)	3.278 (0.023)	3.088 (0.026)	3.008 (0.026)	3.070
	10	3.157 (0.023)	3.028 (0.022)	3.046 (0.024)	3.068 (0.027)	2.976 (0.026)	3.278 (0.023)	3.088 (0.026)	3.008 (0.026)	3.070
Best-of-N	2.982 (0.025)	2.934 (0.027)	2.898 (0.025)	2.930 (0.028)	3.030 (0.027)	3.265 (0.022)	2.966 (0.027)	3.086 (0.023)	3.011	

Table 3: Progress of GEPA across 10 optimization steps from its starting point (Worst5-of-N) and comparison with the BEST-of-N baseline. Each data point, in the mean (standard error) format, indicates the mean and standard error across 411 personas in the test persona set. The last column, labeled “Average”, reports the averages of the means across the eight scenarios.




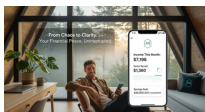
	Odyssey (Electric family SUV)	Oasis (Secluded resort)	Momentum (Mobile banking app)	Aeterno (Luxury watch)	Syncflow (Collaboration tool)
WORST5-OF-64	 Score: 2.828	 Score: 2.839	 Score: 2.644	 Score: 2.942	 Score: 2.641
BEST-OF-64	 Score: 2.966	 Score: 3.265	 Score: 3.030	 Score: 2.982	 Score: 3.086
GEPA (T=10)	 Score: 3.088	 Score: 3.278	 Score: 2.976	 Score: 3.157	 Score: 3.008
T-BoN BO (T=10)	 Score: 3.107	 Score: 3.324	 Score: 3.024	 Score: 3.257	 Score: 3.127

Figure 17: T-BoN BO and baseline’s generated Ad images for five fictional brands: Odyssey electric family SUV (Scenario 3), Oasis eco-lodge (Scenario 4), Momentum Digital Banking (Scenario 5), Aeterno luxury watch (Scenario 7), and SyncFlow B2B software (Scenario 8)

D Proofs

D.1 Auxiliary lemmas

Lemma 3 (Uniform first-order expansion). *Let $g = \nabla\mu(x)$ and $h = \nabla\sigma(x)$. There exist $C > 0$ and $\varepsilon_0 > 0$ such that for all $\varepsilon \in (0, \varepsilon_0]$ and all $u \in \mathbb{R}^d$,*

$$\mu(x + \varepsilon u) = \mu(x) + \varepsilon g^\top u + r_\mu(\varepsilon, u), \quad |r_\mu(\varepsilon, u)| \leq C\varepsilon^2, \quad (28)$$

$$\sigma(x + \varepsilon u) = \sigma(x) + \varepsilon h^\top u + r_\sigma(\varepsilon, u), \quad |r_\sigma(\varepsilon, u)| \leq C\varepsilon^2. \quad (29)$$

Proof. By the mean-value theorem with Lipschitz gradients, for some ξ between x and $x + \varepsilon u$, $\mu(x + \varepsilon u) = \mu(x) + \nabla\mu(\xi)^\top(\varepsilon u)$. Hence $\mu(x + \varepsilon u) = \mu(x) + \varepsilon g^\top u + \varepsilon(\nabla\mu(\xi) - \nabla\mu(x))^\top u$, and $|\nabla\mu(\xi) - \nabla\mu(x)| \leq L_\mu\|\xi - x\| \leq L_\mu\varepsilon$, giving $|r_\mu| \leq L_\mu\varepsilon^2$. The proof for σ is identical with L_σ . Taking $C := \max\{L_\mu, L_\sigma\}$ yields the stated bounds with the same C . \square

Lemma 4 (Max-stability under bounded perturbations). *Let $(f_i)_{i \leq N}$ and $(g_i)_{i \leq N}$ be real arrays. Let $i_f \in \arg \max_i f_i$ and $i_g \in \arg \max_i g_i$. If for some $\Delta \geq 0$,*

$$g_{i_f} \geq f_{i_f} - \Delta \quad \text{and} \quad f_{i_g} \geq g_{i_g} - \Delta, \quad (30)$$

then $g_{i_f} \geq \max_i g_i - \Delta$ and $f_{i_g} \geq \max_i f_i - \Delta$. In particular, $g_{i_f} \geq \max_i g_i - \Delta$ implies that any maximizer of f is a Δ -approximate maximizer of g .

Proof. Since $g_{i_f} \geq f_{i_f} - \Delta = \max_i f_i - \Delta \geq g_{i_g} - \Delta = \max_i g_i - \Delta$, the first claim holds. The second is symmetric. \square

Lemma 5 (Spherical cap coverage). *For $v \in \mathbb{S}^{d-1}$ and $\eta \in (0, 1)$, define $C(v, \eta) := \{u \in \mathbb{S}^{d-1} : v^\top u \geq 1 - \eta\}$. Let $U_1, \dots, U_N \stackrel{i.i.d.}{\sim} \rho$ as above. Then $\max_{i \leq N} v^\top U_i \rightarrow 1$ almost surely as $N \rightarrow \infty$. Moreover, for any deterministic sequence $\eta_N \downarrow 0$ with $N \cdot \rho\{u : v^\top u \geq 1 - \eta_N\} \rightarrow \infty$, we have*

$$\mathbb{P}\left(\max_{i \leq N} v^\top U_i \geq 1 - \eta_N\right) \rightarrow 1. \quad (31)$$

Proof. Let $C(\eta) = \{u \in \mathbb{S}^{d-1} : v^\top u \geq 1 - \eta\}$ be a spherical cap. Since ρ has a density bounded below, $\rho(C(\eta)) \asymp \eta^{\frac{d-1}{2}}$ as $\eta \downarrow 0$. Then $\mathbb{P}(\max_i v^\top U_i < 1 - \eta) = (1 - \rho(C(\eta)))^N \leq \exp(-N\rho(C(\eta)))$. For any fixed $\eta \in (0, 1)$, $\sum_{N \geq 1} \mathbb{P}(\max_i v^\top U_i < 1 - \eta) \leq \sum_{N \geq 1} e^{-N\rho(C(\eta))} < \infty$, so by Borel–Cantelli, $\mathbb{P}(\max_i v^\top U_i < 1 - \eta \text{ i.o.}) = 0$. Intersecting over a countable sequence $\eta_m \downarrow 0$ yields $\max_{i \leq N} v^\top U_i \rightarrow 1$ almost surely. Choosing $\eta_N \downarrow 0$ so that $N\rho(C(\eta_N)) \rightarrow \infty$ yields the result, and taking $\eta = \eta_N \rightarrow 0$ proves the first statement. \square

Lemma 6 (Near-maximum coupling in a thin band). *Let $M_N = \max_i \xi_i$ and define $v_N := (g + M_N h) / \|g + M_N h\|$. Also, $S_i := a_i + b_i M_N$, $Y_i^{(0)} := a_i + b_i \xi_i$, $b_i := \sigma(x) + \varepsilon h^\top U_i$. Fix any sequence $c_N \uparrow \infty$ with*

$c_N/q_N \rightarrow 0$ and set $\delta_N := c_N/q_N$. Then with probability $\rightarrow 1$ there exists an index j such that

$$\xi_j \geq M_N - \delta_N \quad \text{and} \quad v_N^\top U_j \geq 1 - \eta_N, \quad (32)$$

whenever $\eta_N \downarrow 0$ satisfies

$$N \mathbb{P}(\xi \geq M_N - \delta_N) \rho\{u : v_N^\top u \geq 1 - \eta_N\} \rightarrow \infty. \quad (33)$$

Moreover, for this j ,

$$S_j - Y_j^{(0)} = b_j(M_N - \xi_j) \leq b_{\max} \delta_N. \quad (34)$$

Proof. Define $p_{\text{cap},N} := \rho\{u : v_N^\top u \geq 1 - \eta_N\}$ and the event

$$E_N := \{M_N \geq q_N - \delta_N\}. \quad (35)$$

By Lemma 1, $M_N - q_N \rightarrow 0$ in probability and $\delta_N \rightarrow 0$, hence $\mathbb{P}(E_N) \rightarrow 1$.

Set the deterministic threshold $t_N := q_N - 2\delta_N$. On E_N we have $M_N - \delta_N \geq q_N - 2\delta_N = t_N$, hence by monotonicity of the tail,

$$\mathbb{P}(\xi \geq t_N) \geq \mathbb{P}(\xi \geq M_N - \delta_N) \quad \text{on } E_N. \quad (36)$$

Let

$$K_N := \sum_{i=1}^N \mathbf{1}\{\xi_i \geq t_N\} \sim \text{Binomial}(N, p_N), \quad p_N := \mathbb{P}(\xi \geq t_N). \quad (37)$$

A Chernoff bound gives

$$\mathbb{P}\left(K_N < \frac{1}{2} N p_N\right) \leq \exp\left(-\frac{1}{8} N p_N\right). \quad (38)$$

Consider

$$L_N := \sum_{i=1}^N \mathbf{1}\{\xi_i \geq t_N\} \mathbf{1}\{v_N^\top U_i \geq 1 - \eta_N\}. \quad (39)$$

Conditional on $\{\xi_i\}_{i=1}^N$ (and hence on K_N and v_N), the variables $\{\mathbf{1}\{v_N^\top U_i \geq 1 - \eta_N\}\}_{i=1}^N$ are i.i.d. Bernoulli($p_{\text{cap},N}$) and independent of $\{\xi_i\}$. Therefore,

$$L_N \mid \{\xi_i\} \sim \text{Binomial}(K_N, p_{\text{cap},N}), \quad \mathbb{P}(L_N = 0 \mid \{\xi_i\}) = (1 - p_{\text{cap},N})^{K_N} \leq \exp(-K_N p_{\text{cap},N}). \quad (40)$$

We now bound $\mathbb{P}(L_N = 0)$ by splitting on $\{K_N \geq \frac{1}{2}Np_N\}$ and E_N :

$$\begin{aligned}\mathbb{P}(L_N = 0) &\leq \mathbb{E}\left[\exp(-K_N p_{\text{cap},N}) \mathbf{1}_{\{K_N \geq \frac{1}{2}Np_N\} \cap E_N}\right] + \mathbb{P}\left(K_N < \frac{1}{2}Np_N\right) + \mathbb{P}(E_N^c) \\ &\leq \mathbb{E}\left[\exp(-\tfrac{1}{2}Np_N p_{\text{cap},N}) \mathbf{1}_{E_N}\right] + \exp(-\tfrac{1}{8}Np_N) + o(1) \\ &\leq \mathbb{E}\left[\exp(-\tfrac{1}{2}Np_N p_{\text{cap},N})\right] + \exp(-\tfrac{1}{8}Np_N) + o(1).\end{aligned}\tag{41}$$

On E_N , (36) yields $p_N \geq \mathbb{P}(\xi \geq M_N - \delta_N)$. By the lemma's hypothesis,

$$Z_N := Np_N p_{\text{cap},N} \geq N \mathbb{P}(\xi \geq M_N - \delta_N) p_{\text{cap},N} \xrightarrow{p} \infty.$$

Since $0 \leq e^{-\frac{1}{2}Z_N} \leq 1$, for any fixed $T > 0$,

$$\mathbb{E}\left[e^{-\frac{1}{2}Z_N}\right] \leq e^{-\frac{1}{2}T} + \mathbb{P}(Z_N \leq T) \longrightarrow e^{-\frac{1}{2}T}.$$

Letting $T \rightarrow \infty$ gives $\mathbb{E}[e^{-\frac{1}{2}Z_N}] \rightarrow 0$. Moreover, $Z_N \leq Np_N$ since $p_{\text{cap},N} \leq 1$. If Np_N were bounded along a subsequence, then Z_N would be bounded along that subsequence, contradicting $Z_N \xrightarrow{p} \infty$. Hence $Np_N \rightarrow \infty$, so $\exp(-\frac{1}{8}Np_N) \rightarrow 0$. Therefore the second term in (41) vanishes, and $\mathbb{P}(L_N = 0) \rightarrow 0$.

Therefore, with probability tending to one there exists j such that $\xi_j \geq t_N$ and $v_N^\top U_j \geq 1 - \eta_N$. Since $t_N \leq M_N - \delta_N$ on E_N , this j also satisfies $\xi_j \geq M_N - \delta_N$. Finally, $S_j - Y_j^{(0)} = b_j(M_N - \xi_j) \leq b_{\max}\delta_N$ holds deterministically by $M_N - \xi_j \leq \delta_N$ and the definition of b_{\max} . \square

D.2 Proof of Theorem 2

Proof.

By Lemma 3,

$$\begin{aligned}Y_i &= \mu(x) + \varepsilon g^\top u_i + r_\mu(\varepsilon, u_i) + (\sigma(x) + \varepsilon h^\top u_i + r_\sigma(\varepsilon, u_i))\xi_i \\ &= a_i + b_i \xi_i + R_i,\end{aligned}\tag{42}$$

where $a_i := \mu(x) + \varepsilon g^\top u_i$, $b_i := \sigma(x) + \varepsilon h^\top u_i$, and $R_i := r_\mu(\varepsilon, u_i) + \xi_i r_\sigma(\varepsilon, u_i)$. Then $|R_i| \leq C\varepsilon^2(1 + |\xi_i|)$ for all i . Define $S_i := a_i + b_i M_N$, $b_{\max} := \max_{1 \leq i \leq N} |b_i|$, and $U_i := u_i$.

Now let $Y_i^{(0)} := a_i + b_i \xi_i$ and $i_0 \in \arg \max_i Y_i^{(0)}$. From (42),

$$Y_{i^*} \geq Y_{i_0} \implies Y_{i^*}^{(0)} \geq Y_{i_0}^{(0)} - |R_{i^*}| - |R_{i_0}|.$$

By the bound on R_i and $|\xi_i| \leq M_N := \max_j \xi_j$,

$$Y_{i^*}^{(0)} \geq \max_i Y_i^{(0)} - 2C\varepsilon^2(1 + M_N).\tag{43}$$

Symmetrically, $\max_i Y_i^{(0)} \geq Y_{i^*}^{(0)} \geq \max_i Y_i^{(0)} - 2C\varepsilon^2(1 + M_N)$. By Lemma 4, i^* is a $2C\varepsilon^2(1 + M_N)$ -

approximate maximizer of $Y^{(0)}$.

Now let j be the index from Lemma 6 so that $\xi_j \geq M_N - \delta_N$ and $v_N^\top U_j \geq 1 - \eta_N$. By Lemma 3,

$$\max_{i \leq N} S_i - S_j \leq \varepsilon \|g + M_N h\| (1 - v_N^\top U_j) + 2C\varepsilon^2(1 + M_N) \leq \varepsilon \|g + M_N h\| \eta_N + 2C\varepsilon^2(1 + M_N).$$

Also,

$$S_j - S_{i^*} = (S_j - Y_j^{(0)}) + (Y_j^{(0)} - Y_{i^*}^{(0)}) + (Y_{i^*}^{(0)} - S_{i^*}) \leq b_{\max} \delta_N + 2C\varepsilon^2(1 + M_N) + \underbrace{(Y_{i^*}^{(0)} - S_{i^*})}_{\leq 0},$$

where the last term is ≤ 0 provided $b_i \geq 0$ for all i , which holds by Assumption A4 for $\varepsilon \leq \varepsilon_0 := \sigma(x)/(2\|h\|)$ when $\sigma(x) > 0$ since $b_i = \sigma(x) + \varepsilon h^\top U_i \geq \sigma(x) - \varepsilon\|h\| \geq \frac{1}{2}\sigma(x) > 0$. Therefore,

$$\max_{i \leq N} S_i - S_{i^*} \leq \varepsilon \|g + M_N h\| \eta_N + b_{\max} \delta_N + 4C\varepsilon^2(1 + M_N). \quad (44)$$

Set:

$$\Delta'_N(\varepsilon) := b_{\max} \frac{c_N}{q_N} + 4C\varepsilon^2(1 + M_N).$$

By Lemma 3,

$$S_i = \mu(x) + M_N \sigma(x) + \varepsilon(g + M_N h)^\top u_i + \tilde{r}_i, \quad |\tilde{r}_i| \leq C\varepsilon^2(1 + M_N).$$

Hence for any i ,

$$S_i - S_{i^*} = \varepsilon \|g + M_N h\| (v_N^\top U_i - v_N^\top \hat{u}_N) + (\tilde{r}_i - \tilde{r}_{i^*}),$$

so

$$|(S_i - S_{i^*}) - \varepsilon \|g + M_N h\| (v_N^\top U_i - v_N^\top \hat{u}_N)| \leq 2C\varepsilon^2(1 + M_N). \quad (45)$$

Taking i that attains $\max_i S_i$ and using (44) yields

$$\max_{i \leq N} v_N^\top U_i - v_N^\top \hat{u}_N \leq \eta_N + \frac{\Delta'_N(\varepsilon)}{\varepsilon \|g + M_N h\|}. \quad (46)$$

Thus

$$1 - v_N^\top \hat{u}_N \leq \underbrace{1 - \max_{i \leq N} v_N^\top U_i}_{\rightarrow 0 \text{ a.s. by Lemma 5}} + \eta_N + \frac{\Delta'_N(\varepsilon)}{\varepsilon \|g + M_N h\|}. \quad (47)$$

Assume $\|h\| > 0$ (the $\|h\| = 0$ case is addressed in Remark 1). Using

$$\|g + M_N h\| \geq M_N \|h\| - \|g\|$$

and Lemma 1, $M_N \rightarrow \infty$ and $M_N \asymp q_N$. Also $b_{\max} \leq \sigma(x) + \varepsilon \|h\| + C\varepsilon^2$. Hence

$$\frac{\Delta'_N(\varepsilon)}{\varepsilon \|g + M_N h\|} = O_p\left(\frac{c_N}{\varepsilon q_N^2 \|h\|}\right) + O\left(\frac{\varepsilon}{\|h\|}\right).$$

Choosing, e.g., $c_N = \frac{1}{2} \log \log N$ and any $\eta_N \downarrow 0$ with

$$N e^{c_N} \rho\{u : v_N^\top u \geq 1 - \eta_N\} \rightarrow \infty$$

makes the RHS of (47) equal to $o_p(1) + O(\varepsilon)$ for fixed $\varepsilon > 0$; then let $\varepsilon \downarrow 0$.

With $N \rightarrow \infty$ first and fixed $\varepsilon > 0$, (47) implies $1 - v_N^\top \hat{u}_N \xrightarrow{p} 0$. Then $\varepsilon \downarrow 0$ removes the $O(\varepsilon)$ residual, yielding $v_N^\top \hat{u}_N \xrightarrow{p} 1$. Since $M_N - q_N \rightarrow 0$ in probability by Lemma 1, the unit vectors $v_N = (g + M_N h) / \|g + M_N h\|$ and $\tilde{v}_N := (g + q_N h) / \|g + q_N h\|$ satisfy $\|v_N - \tilde{v}_N\| \rightarrow 0$ in probability. Hence $\hat{u}_N \xrightarrow{p} \tilde{v}_N$, which is the claimed gradient direction of A_{β_N} with $\beta_N = q_N$.

By Lemma 3,

$$A_{\beta_N}(x + \Delta x^{(N)}) = A_{\beta_N}(x) + \varepsilon \nabla A_{\beta_N}(x)^\top \hat{u}_N + O(\varepsilon^2).$$

Write $\nabla A_{\beta_N}(x) = g + q_N h$. Using $\tilde{v}_N^\top \hat{u}_N \xrightarrow{p} 1$ gives $\nabla A_{\beta_N}(x)^\top \hat{u}_N = \|\nabla A_{\beta_N}(x)\| \tilde{v}_N^\top \hat{u}_N = \|\nabla A_{\beta_N}(x)\| (1 - o_p(1))$. Thus $A_{\beta_N}(x + \Delta x^{(N)}) \geq A_{\beta_N}(x) + \varepsilon \|\nabla A_{\beta_N}(x)\| - o_p(\varepsilon)$, as claimed. \square

Remark 1 (Edge cases). (i) If $\|h\| = 0$, then $\nabla A_{\beta_N}(x) = g$ and the direction reduces to $\nabla \mu(x)$. (ii) If $\sigma(x) = 0$ but $\|h\| > 0$, the result holds unchanged; only the linearization constants change. (iii) If $\sigma(x) = 0$ and $\|h\| = 0$, the model is locally deterministic and the problem is degenerate; selection aligns with $\nabla \mu(x)$ or is undefined if $g = 0$.

E GP-UCB and its evaluation efficiency

Setup. Let f be a unknown, black-box function that maps a compact and convex feasible region $\mathcal{D} \subset \mathbb{R}^d$ to \mathbb{R} . At each time t , a sampling algorithm \mathcal{A} selects a point $x_t \in \mathcal{D}$ to evaluate. This selection is adaptive, based on the history of previously chosen points and their observed outcomes. The evaluation at x_t yields a noisy observation $y_t = f(x_t) + \epsilon_t$, where ϵ_t is a random noise term, where $\{\epsilon_t : t = 1, 2, \dots\}$ are independent, sub-Gaussian random variables. The unknown function f is assumed to be an element of a Reproducing Kernel Hilbert Space (RKHS), $\mathcal{N}_\Psi(\mathcal{D})$, induced by a stationary kernel Ψ . Functions within this RKHS possess a specific smoothness property, the nature of which is determined by the kernel used. The space $\mathcal{N}_\Psi(\mathcal{D})$ is endowed with an inner product and is formally defined as the set of functions

$$\mathcal{N}_\Psi(\mathcal{D}) := \left\{ g : \mathcal{D} \mapsto \mathbb{R} \mid g(\mathbf{x}) = \sum_{j=1}^{\infty} c_j \Psi(\mathbf{x} - \mathbf{x}_j), \text{ for } \{c_j\} \subset \mathbb{R} \text{ and } \{\mathbf{x}_j\} \subset \mathcal{D} \text{ such that } \|g\|_{\mathcal{N}_\Psi(\mathcal{D})} < \infty \right\}$$

where the norm is given by: $\|g\|_{\mathcal{N}_\Psi(\mathcal{D})} := \left(\sum_{j,l=1}^{\infty} c_j c_l \Psi(\mathbf{x}_j - \mathbf{x}_l) \right)^{\frac{1}{2}}$. For any two functions $g_1(\mathbf{x}) = \sum_{j=1}^{\infty} a_j \Psi(\mathbf{x} - \mathbf{x}_j)$ and $g_2(\mathbf{x}) = \sum_{l=1}^{\infty} b_l \Psi(\mathbf{x} - \mathbf{x}_l)$ in the space, their inner product is $\langle g_1, g_2 \rangle_{\mathcal{N}_\Psi(\mathcal{D})} := \sum_{j,l=1}^{\infty} a_j b_l \Psi(\mathbf{x}_j - \mathbf{x}_l)$. A key feature of RKHS space is the reproducing property, $\langle g, \Psi(\mathbf{x} - \cdot) \rangle_{\mathcal{N}_\Psi(\mathcal{D})} = g(\mathbf{x})$, which holds for all $\mathbf{x} \in \mathcal{D}$. The norm of the function f in this space is assumed to be bounded such that $\|f\|_{\mathcal{N}_\Psi(\mathcal{D})} \leq B$ for some constant $B > 0$.

The objectives. The performance of \mathcal{A} is often evaluated through two types of regret over a time horizon T . One is *cumulative regret*, defined as

$$\mathcal{R}_C(T; f, \mathcal{A}) := \sum_{t=1}^T \left[\max_{\mathbf{x} \in \mathcal{D}} f(\mathbf{x}) - f(\mathbf{x}_t) \right] \quad (48)$$

The other is *simple regret*, defined as

$$\mathcal{R}_S(T; f, \mathcal{A}) := \max_{\mathbf{x} \in \mathcal{D}} f(\mathbf{x}) - f(\mathbf{x}^{(T)}) \quad (49)$$

where $\mathbf{x}^{(T)}$ is the output of the algorithm \mathcal{A} after taking T function evaluations.

The lower bound. Scarlett et al. [2017] showed that a lower bound exists on the regret of *any* algorithm for $f \in \mathcal{N}_\Psi(\mathcal{D})$. Specifically, for any constant $B > 0$,

$$\inf_{\mathcal{A}} \sup_{\|f\|_{\mathcal{N}_\Psi(\mathcal{D})} \leq B} \mathbb{E}[\mathcal{R}_C(T; f, \mathcal{A})] = \begin{cases} \Omega(T^{\frac{\nu+d}{2\nu+d}}), & \text{for Matérn kernels,} \\ \Omega(T^{\frac{1}{2}} \ln^{\frac{d}{2}}(T)), & \text{for SE kernels.} \end{cases} \quad (50)$$

$$\inf_{\mathcal{A}} \sup_{\|f\|_{\mathcal{N}_{\Psi}(\mathcal{D})} \leq B} T(\epsilon, f, \mathcal{A}) = \begin{cases} \Omega\left(\left(\frac{1}{\epsilon}\right)^{2+d/\nu}\right), & \text{for Matérn kernels,} \\ \Omega\left(\frac{1}{\epsilon^2} \left(\log \frac{1}{\epsilon}\right)^{d/2}\right), & \text{for SE kernels.} \end{cases} \quad (51)$$

where Matérn kernels are defined as

$$\Psi_M(\mathbf{x} - \mathbf{x}') := \frac{1}{\Gamma(\nu)2^{\nu-1}} \left(\frac{2\sqrt{\nu} \|\mathbf{x} - \mathbf{x}'\|_2}{\ell} \right)^{\nu} K_{\nu} \left(\frac{2\sqrt{\nu} \|\mathbf{x} - \mathbf{x}'\|_2}{\ell} \right), \quad \mathbf{x}, \mathbf{x}' \in \mathcal{D} \quad (52)$$

and SE kernels are defined as

$$\Psi_{SE}(\mathbf{x} - \mathbf{x}') = \exp\left(-\frac{\|\mathbf{x} - \mathbf{x}'\|_2^2}{2\ell^2}\right), \quad \mathbf{x}, \mathbf{x}' \in \mathcal{D} \quad (53)$$

where $\nu > 0$ is the smoothness parameter, $\ell > 0$ is the length-scale parameter, $\Gamma(\cdot)$ is the gamma function, $K_{\nu}(\cdot)$ is the modified Bessel function of the second kind of order ν , and $\|\cdot\|_2$ denotes the Euclidean norm.

GP-UCB algorithm. The Gaussian Process Upper Confidence Bound (GP-UCB) algorithm, introduced in the seminal work of Srinivas et al. [2012], operates from a Bayesian perspective by placing a Gaussian Process (GP) prior on the unknown objective function f . This GP is characterized by a zero-mean function and a symmetric, positive-definite covariance function, or kernel, $k : \mathcal{D} \times \mathcal{D} \mapsto \mathbb{R}$, where $k(\mathbf{x}, \mathbf{x}') = \Psi(\mathbf{x} - \mathbf{x}')$ for all $\mathbf{x}, \mathbf{x}' \in \mathcal{D}$. For any finite set of points $\{\mathbf{x}_1, \dots, \mathbf{x}_t\} \subset \mathcal{D}$, the corresponding function values $(f(\mathbf{x}_1), \dots, f(\mathbf{x}_t))^{\top}$ are assumed to follow a multivariate normal distribution with a zero mean vector and a covariance matrix with entries $[\mathbf{K}_t]_{jl} = k(\mathbf{x}_j, \mathbf{x}_l)$. Under the assumption of independent, zero-mean Gaussian observation noise with variance σ^2 , conditioning the GP prior on a set of observations $\mathbf{D}_t := \{(\mathbf{x}_j, y_j) : j = 1, \dots, t\}$ yields a closed-form posterior distribution. The posterior mean and variance at any point $\mathbf{x} \in \mathcal{D}$ are given by:

$$\mathbb{E}[f(\mathbf{x}) \mid \mathbf{D}_t] = \mathbf{k}_t^{\top}(\mathbf{x}) \left(\mathbf{K}_t + \sigma^2 \mathbf{I}_t \right)^{-1} \mathbf{y}_t, \quad \text{Var}[f(\mathbf{x}) \mid \mathbf{D}_t] = k(\mathbf{x}, \mathbf{x}) - \mathbf{k}_t(\mathbf{x})^{\top} \left(\mathbf{K}_t + \sigma^2 \mathbf{I}_t \right)^{-1} \mathbf{k}_t(\mathbf{x}), \quad (54)$$

where $\mathbf{k}_t(\mathbf{x})$ is the vector of covariances between \mathbf{x} and the observed points, \mathbf{K}_t is the covariance matrix of the observed points, \mathbf{y}_t is the vector of observed values, and \mathbf{I}_t is the identity matrix. Inspired by upper confidence bound methods in the multi-armed bandit literature (Auer et al., 2002), GP-UCB employs an optimistic acquisition strategy to select subsequent evaluation points. At each step t , the next point \mathbf{x}_{t+1} is chosen by maximizing an upper confidence bound on the function's value $\mathbf{x}_{t+1} = \arg \max_{\mathbf{x} \in \mathcal{D}} \left(\mathbb{E}[f(\mathbf{x}) \mid \mathbf{D}_t] + \sqrt{\beta_t \text{Var}[f(\mathbf{x}) \mid \mathbf{D}_t]} \right)$. This acquisition function naturally balances exploitation, driven by the posterior mean $\mathbb{E}[f(\mathbf{x}) \mid \mathbf{D}_t]$, with exploration, driven by the posterior standard deviation $\sqrt{\text{Var}[f(\mathbf{x}) \mid \mathbf{D}_t]}$. The tunable parameter $\beta_t > 0$ explicitly governs this trade-off, making its specification critical to the algorithm's performance.

The evaluation efficiency of GP-UCB. Whitehouse et al. [2023], Wang et al. [2023a] showed that GP-UCB Srinivas et al. [2012] upper bound on the cumulative regret of *any* algorithm for $f \in \mathcal{N}_\Psi(\mathcal{D})$ that is almost nearly tight. Specifically, for any constant $B > 0$, the GP-UCB algorithm $\mathcal{A}_{\text{GPUCB}}$ achieves

$$\sup_{\|f\|_{\mathcal{N}_\Psi(\mathcal{D})} \leq B} \mathbb{E} [\mathcal{R}_C(T; f, \mathcal{A}_{\text{GPUCB}})] = \begin{cases} O(T^{\frac{\nu+d}{2\nu+d}}), & \text{for Matérn kernels,} \\ O(T^{\frac{1}{2}} \ln^{\frac{d}{2}}(T)) & \text{for SE kernels.} \end{cases} \quad (55)$$

$$\sup_{\|f\|_{\mathcal{N}_\Psi(\mathcal{D})} \leq B} T(\epsilon, f, \mathcal{A}_{\text{GPUCB}}) = \begin{cases} O\left(\left(\frac{1}{\epsilon}\right)^{2+d/\nu}\right), & \text{for Matérn kernels,} \\ O\left(\frac{1}{\epsilon^2} \cdot \left(\log \frac{1}{\epsilon}\right)^{d+3}\right), & \text{for SE kernels.} \end{cases} \quad (56)$$

Wang et al. [2023a]’s approach to proving the regret optimality of GP-UCB follows the two-step framework. The first critical component is to construct a high-probability uniform error bound that quantifies the difference between the true objective function $f(x)$ and its posterior mean estimate $\mu_t(x)$ at any given step t . This bound takes the form $|f(x) - \mu_t(x)| \leq \sqrt{\beta_t} \sigma_t(x)$ for all $x \in \mathcal{D}$, where $\sigma_t(x)$ is the posterior standard deviation and β_t is a carefully chosen exploration parameter. The second component involves bounding the cumulative sum of the instantaneous regrets, which, under the uniform error bound, can be related to the sum of the posterior variances $\sum_{t=1}^T \sigma_{t-1}^2(x_t)$. This sum is, in turn, bounded by the maximal information gain, γ_T . The final regret bound is thus a function of T , β_T , and an upper bound on γ_T . Wang et al. [2023a] employs tools from empirical process theory and decomposes the estimation error, $f(x) - \mu_t(x)$, into a bias term and a random error term. By leveraging the connection between Gaussian process regression and kernel ridge regression, along with properties of the Fourier transform for stationary kernels, they show that the bias term is bounded by $\|f\|_{\mathcal{N}_\Psi(\mathcal{D})} \sigma_t(x)$. The more challenging random error term is handled by viewing it as an empirical process indexed by a class of functions and bounding its supremum. They bound the ϵ -entropy of this function class, which allows for a high-probability bound on the random error. With the new uniform error bound, we can select a much smaller, dimension-independent exploration parameter β_t that grows only logarithmically with T . Combining this sharper β_t with the tightest known bounds on the maximal information gain γ_T for Matérn and SE kernels, we can achieve the tight cumulative regret of GP-UCB.